Location and Diffusion of respiratory gases (O_2 and CO_2) in nano-segregated fluids

João Filipe Viana de Sousa

Thesis to obtain the Master of Science Degree in

Chemical Engineering

Supervisors:

Prof. Dr. Eduardo Morilla Filipe
Prof. Dr. George Jackson

Examination Committee

Chairperson: Prof. Dr. Luísa Martins
Supervisor: Prof. Dr. Eduardo Morilla Filipe
Member of the Committee: Dr. Gonçalo Silva

October 2022

Acknowledgements

First of all, I want to thank Professor Eduardo Morilla, not only for giving me the opportunity to do this thesis under his guidance, but also for the many years of friendship, care and good humour he always showed. My journey through IST wouldn't have been the same without Professor Morilla.

Secondly, I would like to direct a special thanks to Eng. Tiago Eusébio for all the insight he shared with me and for all the time he spent helping me with this thesis whenever I needed it. He was always available to advise me when I felt lost. Without his help this work wouldn't be possible.

I would like to thank Eng. Pedro Silva for his help with some simulation methods, as well as for his willingness to help me. I also want to thank Professor Pedro Morgado for his insightful discussions and suggestions that were crucial for this work.

I want to thank Professor George Jackson for welcoming me and showing me around the Imperial College during my stay in the UK. I'm also thankful for the time he spared to help me and the friendly conversations we had during our meetings.

To my family and friends, I can't thank you enough for all the support you have given me, not only during this thesis, but along all these years that I spent in IST, without you I wouldn't be who I am today.

Abstract

The respiratory gases, oxygen and carbon dioxide in particular, are often said to be fluorophilic as they seem to display enhanced solubilities in perfluorinated solvents. However, this behavior is far from being fully understood, or even confirmed. In this work the subject was addressed using molecular simulations.

Solutions of O_2 and CO_2 in hexane and perfluorohexane at infinite dilution were simulated. The atomistic OPLS-AA force field was used and both molecular dynamics and the Widom particle insertion methods were performed. From the simulation results structural, energetic and transport properties were obtained: solute-solvent interaction energies; solvation enthalpies; Henry's constants; diffusion coefficients; preferential location of the solutes in the pure solvent's structure.

Mixtures of hydrogenated and perfluorinated liquids have been shown to nano-segregate forming distinct hydrogenated and perfluorinated domains. This has been previously demonstrated experimentally using xenon NMR spectroscopy and confirmed by MD simulations. Those results clearly show that the xenon particle is able to detect the existence of such domains, dissolving preferentially in hydrogenated environment. Following the same strategy, in this work infinite dilution solutions of oxygen and carbon dioxide in mixtures of hexane + perfluorohexane and hexanol + perfluorohexanol were also simulated.

From the simulation results no particular interaction or preferential location of O_2 and CO_2 towards perfluorinated solvents could be identified. Thus, any enhanced solubility of the gases in these solvents is probably due to the existence of cavities intrinsic to the liquid structure of the perfluorinated solvents.

Keywords: Molecular Dynamics Simulations, Fluorinated Compounds, Respiratory Gases

Resumo

Os gases respiratórios, em particular oxigénio e dióxido de carbono, são muitas vezes considerados como fluorofílicos pois aparentam ser mais solúveis em solventes perfluorados. No entanto, este comportamento está longe de ser totalmente compreendido ou confirmado. O tópico deste trabalho foi realizado recorrendo a simulações moleculares.

Soluções de O_2 e CO_2 em hexano e perfluorohexano a diluição infinita foram simuladas. O *force field* atomístico usado foi OPLS-AA e recorreram-se aos métodos de dinâmica molecular e de inserção de partículas de Widom. Através das simulações foi possível obter resultados estruturais, energéticos e de propriedades de transporte das soluções: energias de interação soluto-solvente; entalpias de solvatação; constantes de Henry; coeficientes de difusão; localização preferencial dos solutos nos solventes puros.

Em misturas de líquidos hidrogenados e perfluorados já foi mostrada a ocorrência de nano segregação com formação de domínios hidrogenados e perfluorados distintos. Isto foi previamente demonstrado experimentalmente através de espectroscopia de NMR de xénon e confirmado por simulações de dinâmica molecular. Esses resultados mostram claramente que a partícula de xénon consegues detetar a existência de domínios, dissolvendo preferencialmente em ambientes hidrogenados. Seguindo o mesmo procedimento, soluções de oxigénio e dióxido de carbono a diluição infinita em misturas de hexano + perfluorohexano e hexanol + perfluorohexanol também foram simuladas para este trabalho.

Através dos resultados das simulações não foi possível observar uma interação específica ou localização preferencial de O_2 e CO_2 relativamente aos solventes perfluorados. Deste modo, a maior solubilidade dos gases nestes solventes deve-se provavelmente há existência de cavidades intrínsecas da estrutura líquida dos solventes perfluorados.

Palavras-Chave: Simulações de Dinâmica Molecular, Compostos Fluorados, Gases Respiratórios

Contents

List of Tables

List of Figures

Nomenclature

Acronyms

GROMACS - Groningen Machine for Chemical Simulation
H-bonds - Hydrogen Bonds
IE - Interaction Energy
LINCS - Linear Constraint Solver
LJ - Lennard-Jones
MC - Monte Carlo
MD - Molecular Dynamics
MSD - Mean Squared Displacement
OPLS-AA - Optimized Potential for Liquid Simulation All Atom
PME - Particle-Mesh Ewald
RDF - Radial Distribution Function
TPI - Test Particle Insertion

Greek Letters

δ - Phase
ε - Energy Cross Interaction parameter
η - Shear Viscosity; Corrective Factor for the Size Cross Interaction
μ_2 - Chemical Potential of the Solute
ϕ - Torsional Angle
ρ - Density
σ - Size Cross Interaction parameter
θ_0 - Equilibrium Angle
ξ - Corrective Factor for the Energy Cross Interaction; Empirical Corrective Factor for the Diffusion Coefficient
ζ - Friction Coefficient

Roman Letters

a_i - Accelaration of particle i
D - Diffusion Coefficient
ΔH_s - Solvation Enthalpy
H - Henry's Constant
k_a - Equilibrium Bond Length
k_b - Bending Constant
k_B - Boltzmann Constant

m - Mass
M - Molar Mass
n - Number of Minimums and Maximums between 0 and 2π
N - Number of Particles
L - Length of the Box
P - Pressure
q - Atomic Charge
r - Cut-off distance
r_i - Position of particle i
r_{ij} - Distance between the Nuclei
r_0 - Stretching Constant
R - Hydrodynamic Radius/Effective Radii
t - Time
T - Temperature
v_i - Velocity of particle i
V - Volume
V_n - Height of the Potential Barrier
V_M^E - Excess Molar Volume
U - Potential Energy
x - Molar Fraction

Molecules

CO_2 - Carbon Dioxide
F - Fluorine
H - Hydrogen
Hex - Hexane
HexOH - Hexanol
N_2 - Nitrogen
O_2 - Oxygen
OH - Hydroxyl Group
PFH - Perfluorohexane
UFH - Perfluorohexanol
Xe - Xenon

Chapter 1

Introduction

1.1 Perfluorinated Compounds

Fluorine has a very tight bond with its valence electrons, being the most electronegative element, which results in low atomic polarizability and small size. When bonding with carbon atoms, their bond is highly polarized thus making it very strong. This set of characteristics makes it so that fluorine is the only atom that can replace hydrogen in almost any organic molecule [1].

Perfluoroalkanes are organic molecules composed of a saturated carbon chain bonded with fluorine atoms, like regular alkanes but with fluorine instead of hydrogen. This substitution translates to a larger cross-sectional area for the fluorinated chains resulting in higher densities and molar volumes when comparing with their n-alkanes counterparts [2]. When compared to their alkane counterparts, perfluoroalkanes display higher vapour pressures and lower surface tensions due to the low polarizability of the fluorine atom and the weak dispersion forces it creates in the perfluorinated compounds, making them non-flammable compounds with useful applications as fire retardants [3] [4]. Furthermore, there are conformational differences noted between the two chains: the n-alkanes display an all-trans planar form due to their dihedral angle at the energy minimum, while the fluorinated chains present a helical conformation making them rigid in comparison to the hydrogenated chains which have a flexible character. Some authors suggest that the stiffness displayed by the fluorinated chains, due to its less efficient molecular packing, is responsible for the formation of empty spaces between molecules in liquid fluorocarbons, which can explain the higher solubility in respiratory gases shown by perfluoroalkanes [4].

Moreover, the strong C-F bond in perfluoroalkanes and the electronegativity of fluorine leaves the carbon atoms, in fluorinated chains, surrounded by electron rich atoms resulting in few intermolecular interactions and making perfluoroalkanes highly inert and stable compounds. Even though this property can be useful, as it provides many practical applications, it also raises environmental concerns as this stability does not allow an easy natural degradation.

1.2 Mixtures of Hydrogenated and Perfluorinated Compounds

Mixtures of hydrogenated and perfluorinated compounds, in particular, mixtures of alkanes and perfluoroalkanes, despite the very similar intermolecular forces, are known to be highly non-ideal displaying large positive deviations to Raoult's law, very large positive excess volumes, and very large positive excess Gibbs energy and enthalpy [3]. They also display liquid-liquid immiscibility ranges. Perfluoroalkanes and alkanes are mutually phobic. Furthermore, several works demonstrated that perfluoroalkane/alkane mixtures exhibit nano-segregated domains [5] [6]. Mixtures of alkanes and perfluoroalkanes have been extensively studied in past years, however the reason for this mutual phobicity is still poorly understood.

More recently the focus has shifted to the much less documented mixtures of fluorinated and hydrogenated alcohols. The fluorinated alcohols that were object of study in this work are the fluorotelomer alcohols, which are a type of fluorinated alcohols comprised of saturated carbon chains highly fluorinated and a hydroxyl group -OH. These alcohols have a general formula of $CF_3(CF_2)_n(CH_2)_mOH$ (in this work n=5 and m=1). In mixtures of perfluorinated+hydrogenated alcohols, the structure of the liquid results from the balance between preferential hydrogen bonding between the hydroxyl groups of the hydrogenated and fluorinated alcohols and the unfavourable dispersion forces between the hydrogenated and fluorinated chains. With the increase in chain length, the contribution of dispersion increases and eventually overcomes the contribution of the H-bonds, contributing to the segregation between hydrogenated and fluorinated segments [6]. Like perfluoroalkane+alkane mixtures, the mixtures of alcohols display large positive excess molar volumes but, on the other hand, the excess molar Gibbs energy ranges from large and negative to large and positive [6] [7].

1.3 Applications

The interest in studying these fluorinated compounds and their distinctive chemical and mechanical behaviour comes from their wide range of important applications in various fields like medicine or the industry with new applications being discovered every year. In terms of industrial applications, they are used in the production of lubricants, propellants, surfactants, surface coating films (like water and stain repellents), anticorrosives and as cleaning and drying solvents [8] [9] [10]. Moreover, they can also be used in fire extinguishing foams [8] [11] . Although they serve many purposes their main application still is as refrigerants as it is an essential feature in industry and in day-to-day life [8] [12]. For medical purposes, the fluorinated compounds have very important applications as drug delivery agents [13] [14], they also facilitate the transport of oxygen [15] and are used in many anaesthetics [8].

1.4 Motivation for further Investigation

The solubility of respiratory gases in hydrogenated and fluorinated compounds is a prevailing important topic, in particular in the context of carbon capture. CO_2 and O_2 are often said to be more soluble in perfluorinated solvents than their hydrogenated counterparts. However, the subject is far from being fully understood or even proved.

Part of the effect is sometimes justified by the less compact liquid organization of perfluoroalkanes which generates voids in the liquid that small gas molecules can fill [16] [17]. Several studies have been made with the aim of comparing the affinity and interaction of carbon dioxide with fluorocarbons and hydrocarbons. CO_2 is normally modelled placing positive partial charges on the carbon atom and negative partial charges on the oxygen atoms. The molecule can thus behave as a weak Lewis base and as a weak Lewis acid in terms of intermolecular interactions. Raveendran reported that the CO_2 molecule interacts with fluorocarbons through the carbon atom while the interactions with hydrocarbons occur through the oxygen atoms [18]. These studies raised more questions about the preferential affinity of CO_2 molecules for fluorinated or hydrogenated compounds and the results have been conflicting depending on the studied substances. Computational studies by Cece [19] reported positive interaction energies between carbon dioxide and fluorinated molecules and very small interaction energies with hydrogenated molecules. Furthermore, NMR measures made by Dardin [20] also show specific attractive interactions between CO_2 and fluorinated compounds corroborating the previous studies done by Cece. However, infrared [21] and further NMR [22] experiments did not show evidence of a particular interaction between CO_2 and fluorocarbons. Yee [21] reported that the enhanced solubility of fluorocarbons in supercritical CO_2 was due to the highly repulsive fluorocarbon-fluorocarbon interactions favouring solute-solvent interactions. It was also reported by Padua [23], in a computational approach, that there

was no evidence of a particular affinity between fluorocarbons and CO_2. In a recent preliminary study by Monteiro [24] the affinity of CO_2 for hydrogenated and fluorinated alcohols was evaluated at infinite dilution by molecular dynamics simulations, finding no evidence of CO_2 preference for the fluorinated solvents. In conclusion, further investigations on the topic are needed, as well as for other interesting and important respiratory gases such as oxygen and nitrogen.

1.5 Molecular Simulations

Computational simulations, when applied to chemistry, are a very useful resource to help understand and analyse a variety of chemical systems. They can be used to comprehend the structure of systems and their interactions at an atomic level without the restrictions of laboratory experiments. These studies are based on molecular modelling that describe complex chemical systems with the objective of understanding and predicting properties of real systems, serving as a tool that links the microscopic interactions with the real macroscopical behaviour of the systems. These properties can be divided into static equilibrium properties, like density or radial distribution function, and dynamic properties, like viscosity or diffusion coefficients [25].

1.5.1 Theory, Experiments and Molecular Simulations

Molecular simulations are an important resource to complement experimental techniques and theoretical models. While experimental techniques may be useful, they alone might not be able to explain the systems studied with the necessary detail for their understanding. Experimental results allow the development of models that can reproduce these same results. Theoretical models can be devised to mathematically explain the chemical systems so simulations based on these models can then be carried out. The results of the simulations can then be compared to the experimental data to validate the previously devised theoretical model and assess its accuracy. Validated models can then be used to understand and interpret similar systems and future experiments or be used to simulate systems at extreme environments, of temperature or pressure, which are difficult to attain in laboratory conditions [26]. This way it allows us to save resources, money and time. However, besides validating these models, the main goal of molecular simulations is to give detailed information about the physics of the systems like atomic positions, velocities and forces so that they can be understood at molecular level.

1.5.2 Statistical Mechanics

Chemical simulations, as mentioned, are used to give detailed information about the interactions and structure of systems at a molecular level (like atomic positions and velocities) so that the thermodynamic properties (like temperature and pressure) of the same systems can determined. The bridge between mechanical and thermodynamic properties of the systems is based on statistical mechanics. Statistical mechanics deal with average behaviour of a system, some systems are too complex to solve without the use of computer simulations with an accurate molecular model [26] [27].

There are two main technics used to solve the statistical mechanics equations, Monte Carlo and Molecular Dynamics. Monte Carlo method is based on repeated random sampling to obtain numerical results, it is a stochastic method so the dynamic behaviour of the systems can't be precisely calculated [25]. Molecular dynamics is based on finding a numerical solution for the motion equations of the system resulting in more reliable calculations of transport properties and dynamical behaviour [25].

1.5.3 Molecular Dynamics Simulations

Molecular Dynamics is a computational method used to solve Newton's equation of movement, represented by equation 1.1. Where U is the potential energy depending on the position of the N particles of the system. To solve this equation a set of factors must be considered, like, the initial positions and velocities of the particles, the force field, the boundary conditions and the integrators.

$$m_i \frac{d^2 r_i}{dt^2} = -\frac{d}{dr_i} U(r_1, r_2, ..., r_N) \tag{1.1}$$

To numerically solve Newton's equation the leap-frog integrator was used, and it is described by equations 1.2 and 1.3. Where v_i is the velocity of the particle, a_i is the acceleration of the particle and r_i is the position of the particle.

$$v_i(t + \frac{1}{2}\delta) = v_i(t) + \frac{1}{2}\delta t a_i(t) \tag{1.2}$$

$$r_i(t + \delta t) = r_i(t) + \delta t v_i(t + \frac{1}{2}\delta t) \tag{1.3}$$

The velocity of a particle is randomly chosen by a Maxwellian's distribution based on the temperature of the system. The initial position of the particles corresponds to the minimum potential energy configuration of the system.

Another factor to consider are the boundary conditions. In this case as the objective is to calculate bulk properties of the system, periodic boundary conditions were implemented. For these conditions the simulation box is surrounded by an infinite number of replicas, there is no interactions with the walls of the box and when an atom leaves the box from one side it re-enters from the opposite side of the box, this way the number of atoms inside is always constant.

Systems with many molecules tend to take considerably long time to compute because the potential energy of all interactions is calculated. This potential tends to 0 with the increase in distance between particles, so a cut-off distance, r, is defined from which point the potential energy is negligible for the system. This way only the relevant interactions are considered, significantly reducing the computational time of the simulations.

1.5.3.1 Force Field

A force field is a mathematical expression used to characterize the influence and movement of the particles on the energy of the system, describing the intra and intermolecular potential energy of a group of atoms [26]. To build a force field it is necessary to resort to experimental results, semi-empirical quantum mechanics calculations and *ab initio* calculations. The force field can then be optimized by comparing computer simulation results to the thermodynamic properties obtained experimentally. A force field can be described by equation 1.4 [28], where the first three terms represent the bonded parameters, which describe the intramolecular interactions, and the last two terms represent the non-bonded parameters, that describe the intermolecular contributions.

$$U = \sum_{bonds} \frac{1}{2} k_b (r - r_0)^2 + \sum_{angles} \frac{1}{2} k_a (\theta - \theta_0)^2 + \sum_{torsions} \frac{V_n}{2} [1 + cos(n\phi - \delta)] + \sum_{LJ} 4\varepsilon_{ij} \left(\frac{\sigma^{12}}{r^{12}} + \frac{\sigma^6}{r^6} \right) + \sum_{Coulomb} \frac{q_i q_j}{r_{ij}} \tag{1.4}$$

The first term defines the bond stretching, it calculates the length of covalent bonds and is characterized by a harmonic function, where k_b is the bending constant and r_0 is the stretching constant.

The second term defines the angle bending, it calculates the distance between the two external atoms forming the angle, which is also represented by a harmonic function, where k_a is the equilibrium bond length and θ_0 is the equilibrium angle.

For molecules with more than four atoms the torsional term is necessary, it's represented by a cosine function, where ϕ is the torsional angle, δ is the phase, n is the number of minimums and maximums between 0 and 2π and V_n is the height of the potential barrier.

The intermolecular terms described in equation 1.4 are the Van der Waals and the electrostatic interactions. The fourth term determines the 12-6 Lennard-Jones (LJ) potential, that represents the balance between repulsive and attractive forces. The attractive forces arise from the induced dipoles and the repulsive forces are generated by the overlap of electron clouds of the atoms [25]. ε is the minimum potential energy and measures the attraction strength of two particles. σ is the distance at which the potential between particles is zero and defines how close two non-bonded particles can get. These parameters are calculated by geometrical mean rules for both energy and size described by equations 1.5 and 1.6.

$$\varepsilon_{ij} = \sqrt{\varepsilon_{ii} \cdot \varepsilon_{jj}} \tag{1.5}$$

$$\sigma_{ij} = \sqrt{\sigma_{ii} \cdot \sigma_{jj}} \tag{1.6}$$

The last term defines the electrostatic or Coulombic interactions, this term results from the unequal distributions of charges in a molecule [29], where q represents the atomic charges and r_{ij} is the distance between the nuclei.

1.6 Studied Systems and Objectives

The objectives of this work were to study and compare the affinity of respiratory gases, in particular CO_2 and O_2, in hydrogenated and fluorinated solvents and their mixtures, using molecular dynamics simulations as a tool. The location and diffusion of the solutes at infinite dilution conditions were analysed.

The solvents chosen were perfluorohexane, hexane, perfluorohexanol and hexanol. The pure solvents and mixtures were first simulated and their densities and excess molar volumes calculated to assess the accuracy and validity of the simulations in reproducing known experimental data. Through the analyses of the radial distribution functions between the hydrogen and fluorine atoms, the structure of the liquid mixtures was obtained confirming the existence of nano-segregated domains.

The Widom particle insertion method was used to estimate the Henry's constants and solubility of Xe, CO_2 and O_2 in hexane and perfluorohexane at several temperatures. Solutions of CO_2 and O_2 in the hydrogenated and fluorinated solvents and their mixtures at infinite dilution conditions were then simulated. RDFs between the probe molecules and the hydrogenated and fluorinated compounds were computed to determine the preferential location of O_2 and CO_2. Interaction energies and solvation enthalpies of the respiratory gases with the solvents were also calculated to evaluate the affinity between the solutes and both solvents. To retrieve information regarding the dynamics of O_2 and CO_2 solutions, their diffusion coefficients and hydrodynamic radius in the mixtures were calculated through the mean squared displacement functions.

Chapter 2

Simulation Procedure

Molecular dynamics simulations were performed to get a better understanding of the behaviour of CO_2 and O_2 molecules at infinite dilution in systems of fluorinated and hydrogenated solvents. For this study two alkanes were used, Perfluorohexane (PFH) and Hexane (Hex), as well as two alcohols, Perfluorohexanol (UFH) and Hexanol (HexOH).

To run all the molecular dynamics simulations an open-source package of GROMACS (Version 2018) [30] [31] was used. The systems of molecules were fit in cubic boxes with periodic boundary conditions for all directions and a time step of 2 fs. The simulations were performed in boxes containing 300 molecules of solvent and 1 molecule of either CO_2, O_2 or Xe, maintaining the system size and changing the ratio of fluorinated to hydrogenated solvent. The systems that analysed the behaviour of the pure solvents to facilitate the determination of the solvation energy were composed of only 300 solvent molecules.

To carry out the molecular simulations the following procedure was performed:

1st – A box was generated containing the necessary molecules all randomly placed. The box was then submitted to an energy minimization phase for 20000 steps without temperature or pressure control, bringing the system to a lower energy state.

2nd – The resulting box from the first step was then submitted to an equilibration phase in NPT (meaning the number of particles, pressure and temperature are specified) ensemble for 1 ns and 500000 steps at a temperature of 600K and a pressure of 200 atm. During this stage the temperature and pressure were controlled with the Beredensen thermostat and barostat.

3rd – The box was then submitted to the production step in NPT ensemble for 30 ns, to get good statistics of the behaviour of the probe molecules in the mixtures, or 100 ns only for the simulations where potential energy values with low uncertainty were needed (due to the high amount of disk space they occupy). This step was done at 1 atm and at three different temperatures, 283.15 K, 298.15 K and 313.15 K to study the influence of temperature in some properties. During this stage the pressure was controlled with the Parrinello-Rahman barostat [32], and the temperature was controlled with the Nosé-Hoover thermostat [33].

To be able to perform these simulations it was necessary to choose a force field that contains the information of all the interactions between the particles of the systems. In this case the models used were OPLS-AA, the atomistic optimized potential for liquid simulations all-atom [34] [35] and the L-OPLS-AA [36] which is an extension of the former force field but for longer hydrocarbon chains. The parameters used for Hexanol and Hexane molecules are published on papers [37] [36]. For the fluorinated chains more parameters were needed to complete the force field and simulate their behaviour realistically. To describe the CF_3-CF_2 interactions the parameters were taken from the OPLS-AA work on perfluoroalkanes [35], for the CF_3-CF_2-OH interactions the force field parameters were developed by

Duffy [38]. The remaining dihedral torsion parameters were obtained from work [39] by Padua. The parameters of the CO_2 molecule were obtained from a paper by Harris and Yung [40], for the O_2 molecule the parameters were taken from a paper by Miyano [41] and for Xe the paper by Fischer and Kohler [42] was used.

The non-bonded parameters implemented on the force field used for the construction of the molecules studied are displayed in table 2.1.

Table 2.1: Non-bonded parameters in the force field used for the construction of Hex, HexOH, PFH, UFH, CO_2, O_2 and Xe.

Name	Bond Type	M	q	ε	σ
opls_099	Xe	131.2930	0.000	0.3950	1.894000
opls_135	CT	12.0110	-0.180	0.3500	0.276144
opls_136	CT	12.0110	-0.120	0.3500	0.276144
opls_140	HC	1.0080	0.060	0.2500	0.125520
opls_154	OH	15.9994	-0.683	0.3120	0.711280
opls_155	HO	1.0080	0.418	0.0000	0.000000
opls_157	CT	12.0110	0.145	0.3500	0.276144
opls_160	CT_4	12.0110	0.126	0.3500	0.276144
opls_161	CTF	12.0110	0.532	0.3250	0.259408
opls_162	OH	15.9994	-0.635	0.3070	0.711280
opls_163	HO	1.0080	0.429	0.0000	0.000000
opls_164	F	18.9984	-0.206	0.2940	0.255224
opls_165	HC	1.0080	0.083	0.2500	0.125520
opls_961	CTF	12.0110	0.360	0.3500	0.276144
opls_962	CTF	12.0110	0.240	0.3500	0.276144
opls_965	F	18.9984	-0.120	0.2950	0.221752
opls_966	CTL	12.0110	-0.222	0.3500	0.276144
opls_967	CTL	12.0110	-0.148	0.3500	0.276144
opls_968	HTL	1.0080	0.074	0.2500	0.125520
opls_969	HTL	1.0080	0.074	0.2500	0.110000
co2_1	CO	12.0110	0.6512	0.2757	0.233900
co2_2	OC	15.9994	-0.3256	0.3033	0.669400
oo	OO	15.99	0.00	0.3030	0.4015662

Another important thing to consider is the, already mentioned, non-bonded Lennard-Jones interactions between different types of sites, these are calculated by geometrical mean rules for both energy and size, equations 1.5 and 1.6 respectively.

These energy and diameter cross-interactions are not properly designed for the weak unlike interactions between the hydrogenated and fluorinated chains in the mixtures [43] to replicate experimental excess properties. So, some corrections were made by adding a corrective factor to each of these parameters. For the energy cross-interaction a factor of ξ=0.77 was implemented and for the size cross-interaction the factor was η=1.035, these were suggested by Morgado et al. for the L-OPLS-AA force field [6] [44]. This way, by multiplying the corrective factors by their respective equation, the force field parameters are adjusted for the mixtures of fluorinated and hydrogenated compounds.

For the same molecule, only atoms separated by three or more bonds are considered for the non-bonded interactions between atoms. Both Lennard-Jones and the long-range electrostatic (Coulomb) interactions were truncated by using cut-offs of 14 Å. To calculate the long-range Coulomb interactions, beyond the cut-off, the Particle-Mesh Ewald (PME) method was used. All bonds involving Hydrogen

atoms were considered as rigid by being restricted to their equilibrium lengths, using the LINCS algorithm [45]. For all simulations, a neighbour list with a radius of 10 Å was used and updated every 10 steps.

To determine the Henry's constant and solubility of Xe, CO_2 and O_2 in the solvents the test-particle insertion (TPI) method was used [46]. To use this method a simulation box with only the pure solvent was created according to the three previously described steps. The box, using the TPI logarithm, is then submitted to multiple random insertions of the solute molecule, in this case 1000 insertions per frame with a radius of insertion of 0.02 nm.

2.1 Calculation of Thermodynamic, Structural and Dynamic Properties from MD Simulations

After completing all the simulations, it was possible to calculate the properties of the systems. Since the production step of the simulations was done in NPT, the densities of the mixtures were obtained directly from the average volume of the box. The excess molar volume of the mixtures was calculated through equation 2.1 where x is the molar fraction, M represents the molar mass and ρ is the density.

$$V_M^E = \frac{x_1 M_1 + x_2 M_2}{\rho} - \frac{x_1 M_1}{\rho_1} - \frac{x_2 M_2}{\rho_2} \tag{2.1}$$

The Henry's constant was calculated through equation 2.2 where μ_2 is the chemical potential of the solute, determined by GROMACS using the TPI method, ρ_1 is the density of the solvent, R is the ideal gas constant and T is the temperature of the solution.

$$H_{2,1} = \lim_{x_2 \to 0} \left[RT\rho_1 \cdot exp\left(\frac{\mu_2^r}{RT}\right)\right] \tag{2.2}$$

The solvation enthalpies of Xe, CO_2 and O_2 were calculated through the difference between the potential energy of the solution, for each solute, and the potential energy of the solvent. The potential energy was obtained directly from GROMACS.

To analyse the solvent structure and to check the preferred location of the CO_2 and O_2 molecules in the mixtures, the method chosen was to compute the radial distribution functions (RDFs) which determine the density of probability of finding a particle at a distance r from a reference particle, equation 2.3.

$$g(r) = \frac{1}{N\rho} \sum_{i}^{N} \sum_{j \neq i} \delta(r - r_{ij}) \tag{2.3}$$

First, the RDFs were performed between the fluorinated and hydrogenated solvents to study the solvent structure of the mixtures, then they were performed between the solute molecules and the solvents to identify the preferred location of CO_2 and O_2 molecules.

Using the RDFs, another parameter that was determined was the local composition around the solute molecules. It was necessary to determine the number of fluorine and hydrogen neighbours for each solute molecule through the RDFs and cumulatives of the interactions solute-F and solute-H . The distance considered to calculate the number of neighbours was the relative minimum of the solute-F RDF, since fluorine is bigger than hydrogen. With the number of neighbours taken from the RDF's cumulatives it was possible to calculate the local composition of the mixtures from the ratio between the number of fluorine neighbours and the total number of neighbours.

The diffusion coefficients for Hex, HexOH, PFH, UFH, CO_2 and O_2 in the mixtures studied at different compositions were calculated using the Einstein equation 2.4.

$$D_0 = \frac{1}{6N} \lim_{t\to\infty} \frac{d}{dt} \sum_{N}^{i=1} \left\langle |r_i(t) - r_i(0)|^2 \right\rangle \tag{2.4}$$

In equation 2.4, $|r_i(t) - r_i(0)|^2$ is the mean squared displacement of a single solute molecule averaged over time. To calculate the diffusion coefficient through the simulations, first the mean squared displacement was computed for intervals of 5 ns for all 30 ns of the simulations. Then the slope of the linear part of the MSD function was determined for each interval. The mean value of the slopes was then calculated resulting in the diffusion coefficient. Since the Einstein equation doesn't consider the the size of the simulation box, a corrective factor [47] was applied in equation 2.5 resulting in the corrected diffusion coefficient. Where k_B is the Boltzmann constant [48], T is the temperature of the simulations, ξ is an empirical factor of 2.837297 [47], L is the length of the box and η is the viscosity of the solvent.

$$D = D_0 + \frac{k_B T \xi}{6\pi\eta L} \tag{2.5}$$

The viscosities used for the PFH+Hex mixture were the experimental data obtained by Morgado shown in paper [2] and for the mixture of UFH+HexOH the experimental viscosities were taken from work [49] by Miguel Costa.

The translational movement of a solute in a fluid at infinite dilution can be described by the Einstein equation 2.6 where ζ is the friction coefficient.

$$D = \frac{k_B T}{\zeta} \tag{2.6}$$

At the hydrodynamic limit of a sphere diffusing in a fluid it's possible to deduce the Stokes-Einstein equation 2.7, where C is determined by the boundary conditions, in this case 6.

$$D = \frac{k_B T}{C\pi\eta R} \tag{2.7}$$

The hydrodynamic radius, R, was then calculated through the equation of Stokes-Einstein 2.7, using the diffusivities previously determined and the experimental viscosities taken from the literature already cited.

The interaction energies between the respiratory gases and the solvents were calculated by the sum of the Coulomb and Lennard-Jones interaction energies, which were obtained directly from GROMACS.

Chapter 3

Results and Discussion

3.1 Mixtures of Hydrogenated and Fluorinated Solvents

3.1.1 Densities and Excess Molar Volumes: Force Field Validation

For this study the densities and excess molar volumes of the mixtures (Hex+PFH) and (HexOH+UFH) were calculated at 298.15K and atmospheric pressure, to assess if the simulations are a good representation of reality. The solvent mixtures should have been simulated without any solute particles (CO_2 or O_2). However it was considered that the presence of a single molecule of CO_2 or O_2 would not affect significantly the properties of the solvent mixtures. Therefore, the following results for the solvent properties were obtained from simulations that include a molecule of solute.

In figure 3.1 the densities of (Hex+PFH) mixtures are plotted and compared to experimental data [50]. The simulated densities of (HexOH+UFH) mixtures displayed in figure 3.2 are compared with experimental data [51].

The excess molar volumes are plotted in figure 3.3 for Hex+PFH mixtures where they are compared with experimental values [50]. For HexOH+UFH mixtures the excess molar volumes are presented in figure 3.4 and are also compared to experimental data [51].

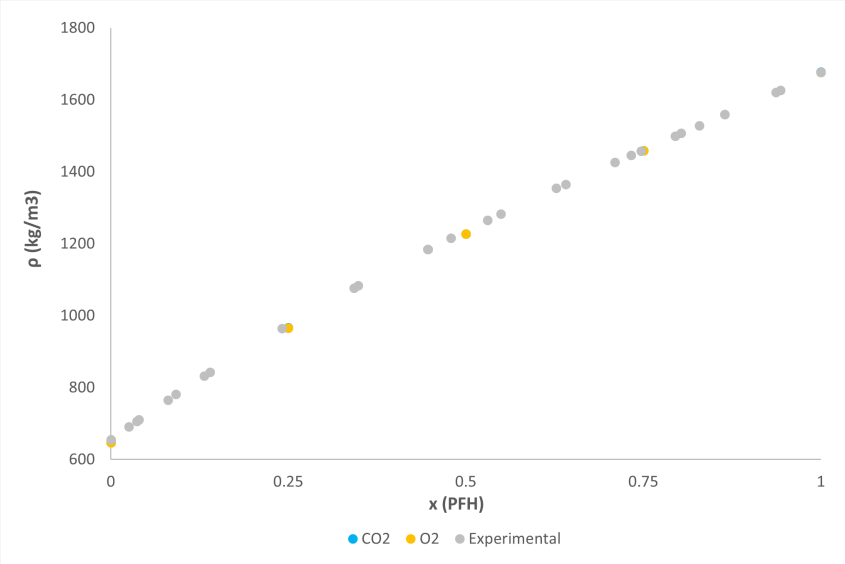

Figure 3.1: Densities of Hex+PFH mixtures at 298.15 K and atmospheric pressure. Blue - simulations with CO_2; Yellow - simulations with O_2; Grey - experimental data.

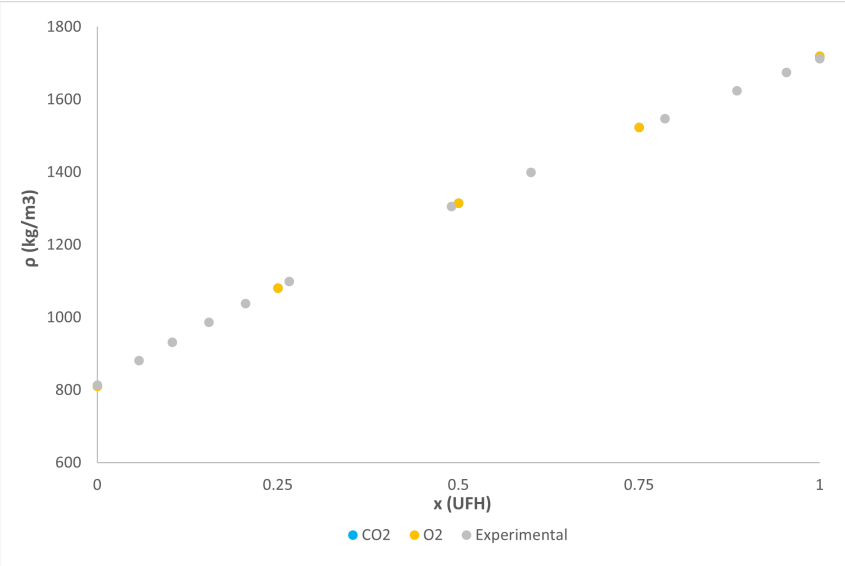

Figure 3.2: Densities of HexOH+UFH mixtures at 298.15 K and atmospheric pressure. Blue - simulations with CO_2; Yellow - simulations with O_2; Grey - experimental data.

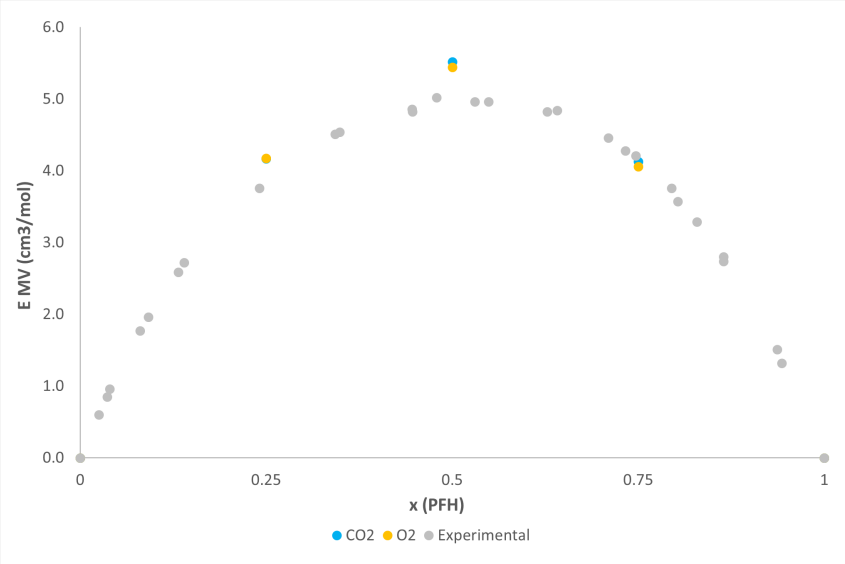

Figure 3.3: Excess molar volumes of Hex+PFH mixtures at 298.15 K and atmospheric pressure. Blue - simulations with CO_2; Yellow - simulations with O_2; Grey - experimental data.

As can be seen, the densities and excess molar volumes obtained from MD simulations agree with the experimental data. As previously mentioned, it has been shown in previous studies that the unlike interactions between the hydrogenated and fluorinated chains must be corrected relatively to the geometric mean rule. With these corrections ξ = 0.77 and η = 1.035 [5] the simulations reproduce well the experimental densities of the mixtures and even their excess molar volumes. It is important to understand that the prediction of excess molar volumes is a difficult test to any computational method so by obtaining matching results with experimental data it assures us that these models are very good at representing the interactions within the systems and so it allows us to consider more seriously results that don't have experimental data to compare.

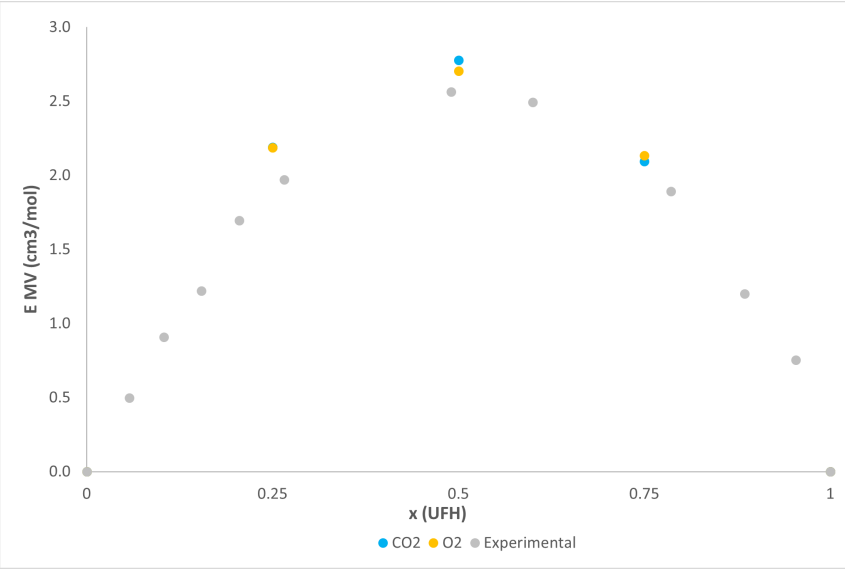

Figure 3.4: Excess molar volumes of HexOH+UFH mixtures at 298.15 K and atmospheric pressure. Blue - simulations with CO_2; Yellow - simulations with O_2; Grey - experimental data.

3.1.2 Liquid Structure of (Hydrogenated+Fluorinated) Mixtures

To study the liquid structure of the PFH+Hex and UFH+HexOH systems the radial distribution functions (RDFs) were computed. These were obtained from the trajectory of the simulations and were used to better understand the interactions between the different molecules in the mixtures. The RDFs generated for the Hex+PFH and HexOH+UFH are displayed in figures 3.5 and 3.6, respectively.

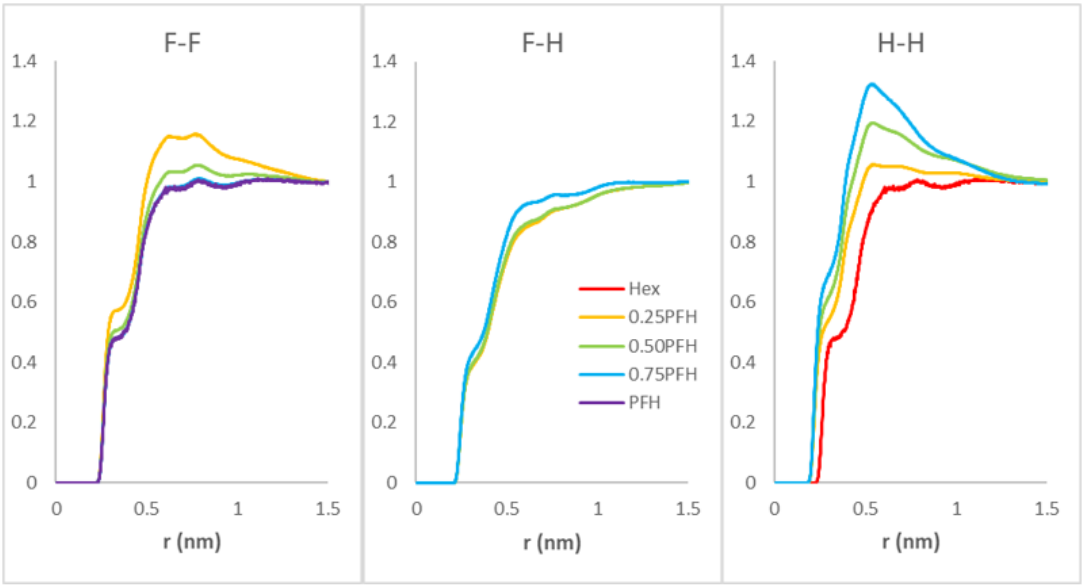

Figure 3.5: Intermolecular RDFs between hydrogen and fluorine atoms at 298.15K for mixtures of Hexane and PFH at different compositions; Red - Hexane; Yellow - 0.25 PFH; Green - 0.5 PFH; Blue - 0.75 PFH; Purple - PFH.

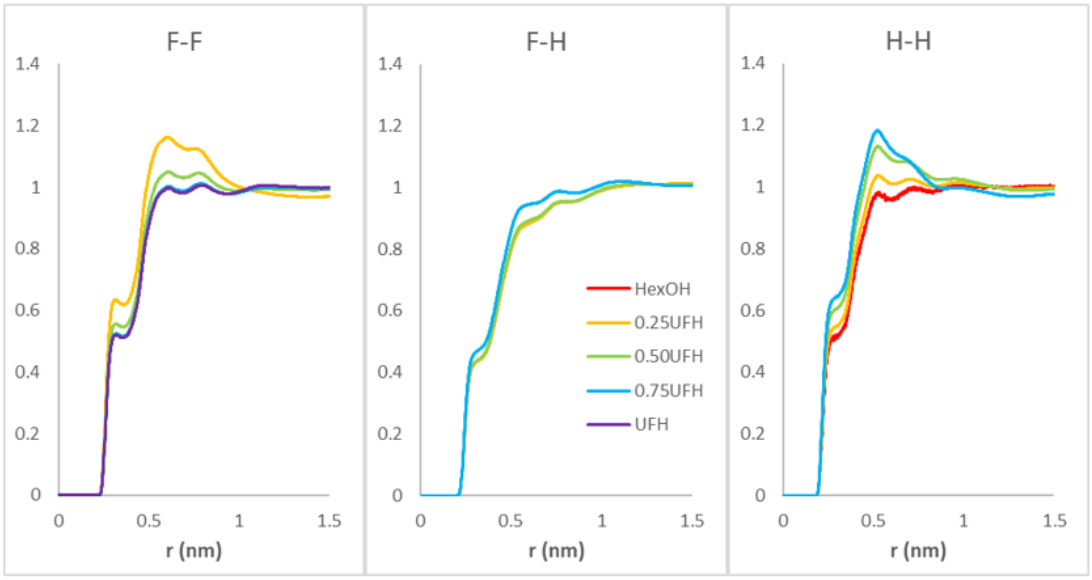

Figure 3.6: Intermolecular RDFs between hydrogen and fluorine atoms at 298.15K for mixtures of Hexanol and UFH at different compositions; Red - Hexanol; Yellow - 0.25 UFH; Green - 0.5 UFH; Blue - 0.75 UFH; Purple - UFH.

As can be seen, the RDFs between hydrogenated and fluorinated chains have low intensity for all mixtures, which means there is a lower probability of them being neighbours, leaning towards nano-segregation of the hydrogenated and fluorinated molecules and formation of domains. The intensity of the F-F peaks increases with the increase in hydrogenated compound concentration. The reverse happens to the intensity of the H-H peaks, it increases with the fluorinated compound concentration. This was verified for alkanes and alcohols alike. This is an indication that fluorinated chains are mainly surrounded by fluorinated chains and that hydrogenated chains are mainly surrounded by hydrogenated chains. These results seem to prove the existence of fluorinated and hydrogenated domains, as can be seen in figure 3.7 that shows a snapshot of the simulations ran for the equimolar mixtures. Finally, it's also worth to compare both alkane and alcohol mixtures. The alkane RDF peaks of H-H and F-F interactions are more intense than the same peaks of the alcohol mixtures, and the peaks of F-H interactions are lower in the alkane mixtures, indicating that there is a higher degree of nano-segregation in the alkane mixtures. The results from work [5] by Morgado et al., where xenon NMR spectroscopy and MD simulations were used, support the results from this study.

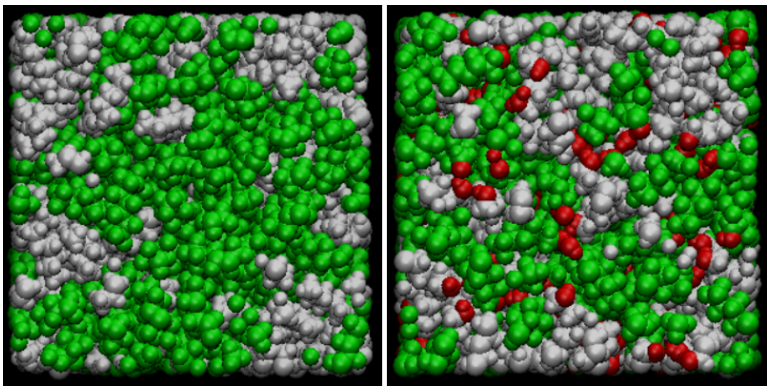

Figure 3.7: Snapshot of MD simulation boxes of two equimolar mixtures, Hex+PFH on the left and HexOH+UFH on the right; Green - PFH and UFH; White - Hexane and Hexanol; Red - Hydroxyl group.

3.2 Solutions of Xe, CO_2 and O_2: Parametrization of Solute-Solvent Cross Interactions

3.2.1 Solubility and Henry's Constant

As previously mentioned the TPI method was used to calculate the Henry's constants of Xe, CO_2 and O_2, at atmospheric pressure and three different temperatures (10ºC, 25ºC and 40ºC), to study their solubilities in Hexane and Perfluorohexane. Xenon was included in the study as a comparison particle as it has been extensively studied in our research group. The results are shown in figures 3.8, 3.9 and 3.10. For Xe the results are compared to experimental data obtained by Pollack et al. [52] [53] and to previous simulations done by Pádua et al. [54]. For CO_2 the TPI method results are compared to previous simulations done by Pádua et al. [23]. The O_2 simulation results are compared to experimental data obtained by Pádua et al. [55].

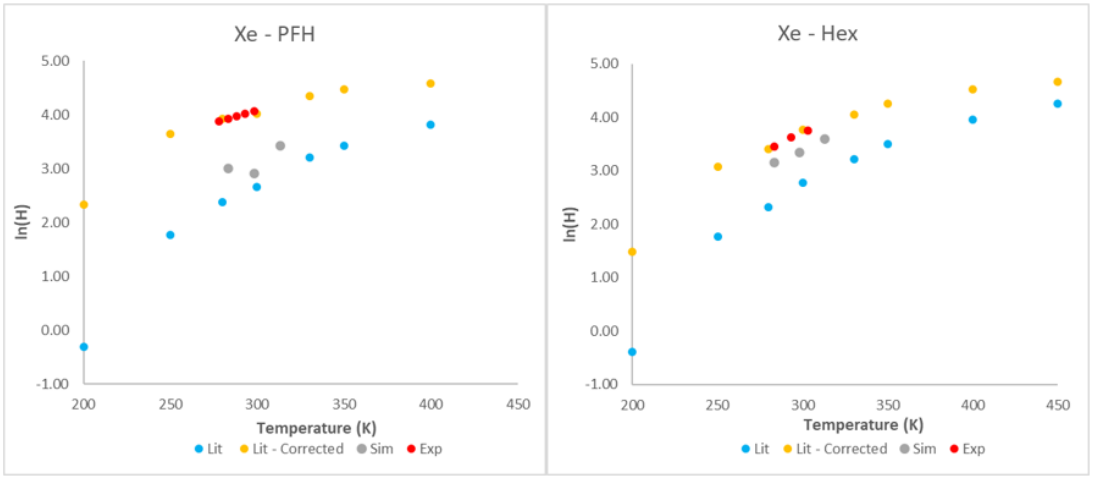

Figure 3.8: Henry's Constant for Xe in perfluorohexane (left) and hexane (right) at different temperatures and atmospheric pressure. Blue - simulations by Pádua et al.; Yellow - simulations with adjusted energy interaction parameter by Pádua et al.; Grey - simulation results; Red - experimental data by Pollack et al.

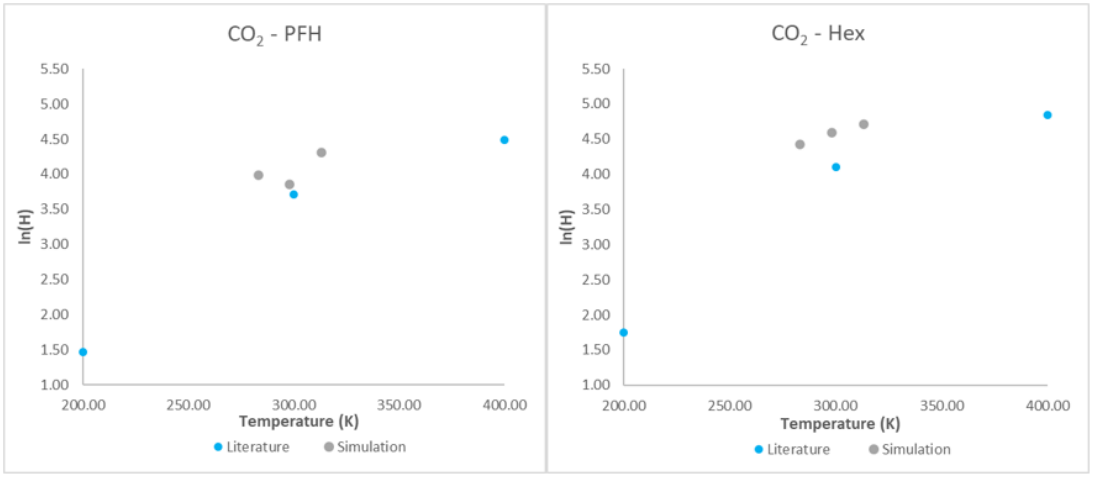

Figure 3.9: Henry's Constant for CO_2 in perfluorohexane (left) and hexane (right) at different temperatures and atmospheric pressure. Blue - simulations by Pádua et al.; Grey - simulation results.

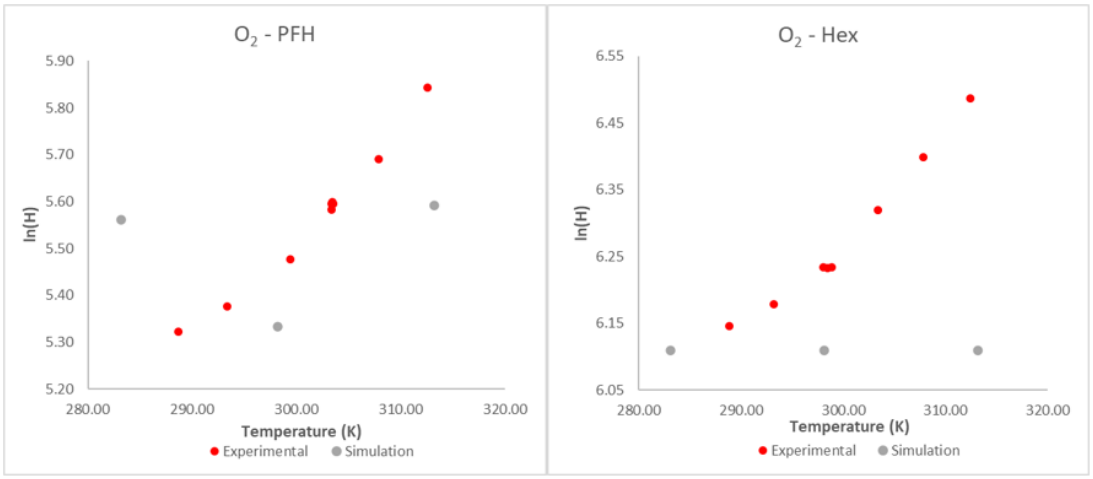

Figure 3.10: Henry's Constant for O_2 in perfluorohexane (left) and hexane (right) at different temperatures and atmospheric pressure. Red - experimental data by Pádua et al.; Grey - simulation results.

As can be seen, from figure 3.8 the experimental solubilities of Xenon are higher in hexane than in perfluorohexane, as the Henry's constant is inversely proportional to solubility. The simulated results of Xe in hexane seem to replicate well enough the experimental results. However the simulated solutions of Xe in PFH present a positive deviation of solubility when compared to the experimental results. This can be an indication that the energy cross interaction parameter between xenon and PFH needs to be slightly decreased. Pádua used a correction to the unlike energy parameter between xenon and PFH ξ=0.820, so a similar correction should be used in our case.

From figure 3.9 it's possible to see that CO_2 is more soluble in PFH than in hexane. The solubilities calculated for CO_2 are close to those obtained by Pádua et al. [23]. There is no experimental data for this mixture but it's possible to compare the ratio of solubilities PFH/Hex to the experimental ratio of perfluoroheptane/heptane [23]. For the mixture of PFH+Hex the determined ratio is around 1.71 and for the mixture of perfluoroheptane+heptane it's around 1.73 [23]. As there is no evident reason for the ratios to be different, since the molecules in question are very similar in size and properties, it is an indication that similar adjustments would be needed for the cross interactions between CO_2 and the two solvents. Since there is no experimental data for the solubility of CO_2 in each solvent, it is not possible to conclude if corrections for the cross interaction are needed.

As for O_2, it can be seen from figure 3.10 that the simulated solubilities show a positive deviation when compared to the experimental data, with the exception of the solubility of oxygen in PFH at 10ºC which shows a negative deviation. Although the simulated solubilities of O_2 reproduce quite well the experimental data, a slight adjustment to the energy cross interactions between O_2 and the solvents might be needed. However, this conclusion is difficult considering the uncertainty of the simulation results. Performing more simulations at more temperatures would be advisable. When comparing the solubilities of the three solutes it's possible to see that Xe has the highest solubility followed by carbon dioxide, oxygen has the lowest solubility.

3.2.2 Solvation Enthalpy

The solvation enthalpies of Xe, CO_2 and O_2 in hexane and PFH were calculated at atmospheric pressure and at different temperatures, the results are displayed in figure 3.11. For CO_2 no experimental data was found to compare the simulation results.

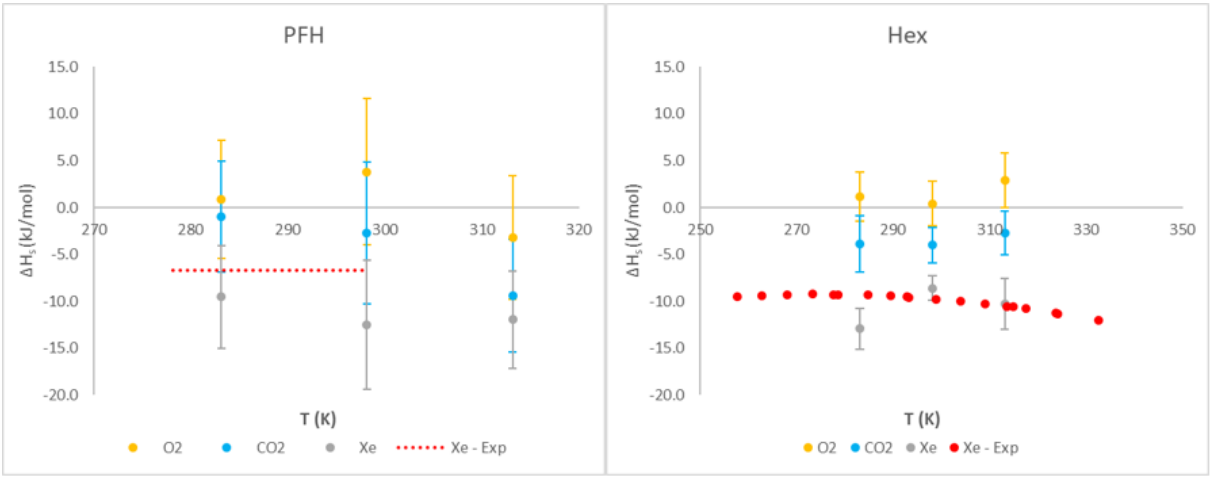

Figure 3.11: Simulated solvation enthalpy of Xe (Grey), CO_2 (Yellow) and O_2 (Blue) at different temperatures and atmospheric pressure, in perfluorohexane (left) and hexane (right). Experimental $\Delta\bar{H}_s$ of Xe in PFH (Red dotted line) and experimental ΔH_s of Xe in hexane (Red).

As can be seen from figure 3.11, for both solvents, Xe has the largest (more negative) solvation enthalpy followed by CO_2 and then O_2. The simulated solvation enthalpies of Xe in hexane reproduce well the experimental results obtained by Martins et al. [56], which is a good indication that the simulations performed are a good representation of the real behaviour of the solutions and the energy interaction parameter between Xe and Hex does not need to be adjusted. For Xe in PFH, Pollack et al. [53] determined the mean solvation enthalpy, $\Delta\bar{H}_s$, between 5ºC and 25ºC, represented by the dotted red line in figure 3.11, which fits within the standard deviation of our simulation results indicating that a slight adjustment of the parameters might be needed. According to Pádua et al. [55], the experimental solvation enthalpies of O_2 vary between 0 and -26 kJ/mol in a short range of temperatures, around 30ºC. This change, from an essentially athermic solvation energy to a highly exothermic one, in such a short range of temperatures, does not seem very physically realistic. However, it's clear that the $\Delta\bar{H}_s$ might be negative in both solvents with a mean value in the order of -10 kJ/mol to -12.5 kJ/mol, being difficult to conclude in which solvent the solvation enthalpy is more exothermic. The simulation results are practically 0 within the statistical error, which seems to indicate a need to increase the cross energy interaction between O_2 and both solvents. Once again it's difficult to decide which solvent needs the larger adjustment to its cross interaction parameter considering the statistical error and how large should those adjustments be considering the experimental data available. For CO_2 no adjustment was considered as there is no experimental ΔH_s to guide it and as mentioned in chapter 3.2.1 the calculated solubilities seem to agree with the experimental results available.

3.3 Solutions of CO_2 and O_2 in (Hydrogenated+Perfluorinated) Mixtures

To get insight on the location of CO_2 and O_2 in the binary mixtures of PFH+Hex and UFH+HexOH RDF analyses of these systems were performed. The nomenclature, used in this work, to identify the carbon atoms is displayed in figures 3.12 and 3.13 for the PFH and UFH molecules, their hydrogenated counterparts have the same carbon numbers. The fluorinated carbons are referred as 'CFi' to distinguish them from the hydrogenated carbons, identified as 'Ci'.

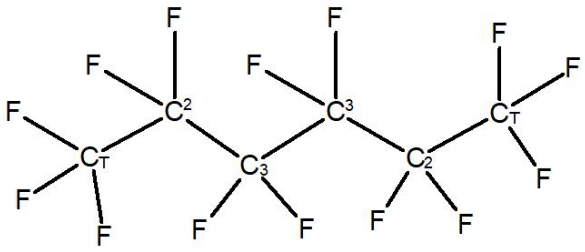

Figure 3.12: Molecular formula of Perfluorohexane with the nomenclature used to identify the carbon atoms.

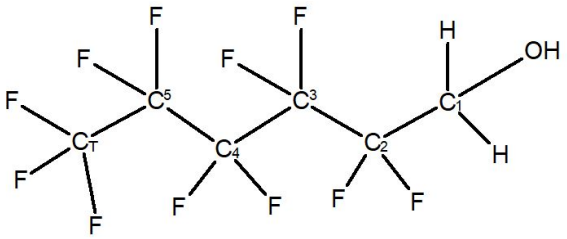

Figure 3.13: Molecular formula of Perfluorohexanol with the nomenclature used to identify the carbon atoms.

3.3.1 Location of CO_2 and O_2 in Pure Hydrogenated and Perfluorinated Solvents

First, for the solutions containing one carbon dioxide molecule in the pure solvents, replicating an infinite dilution situation, RDFs were computed at 298.15K. Figures 3.14 and 3.15 show the RDFs obtained. For these RDFs the analyses were performed between the carbon of the carbon dioxide molecule and the carbons of the hydrogenated and fluorinated chains. In the case of UFH and HexOH, the RDFs between the carbon of CO_2 and the oxygen of the hydroxyl group were also included.

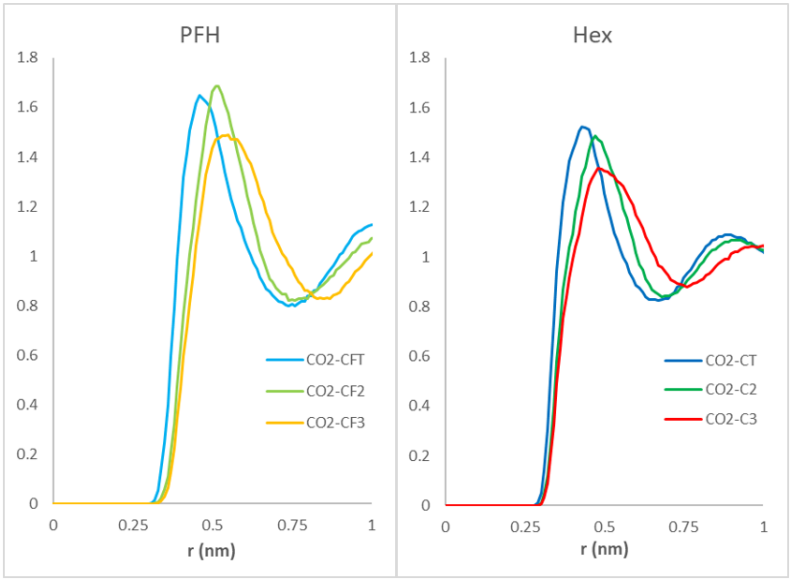

Figure 3.14: RDFs between the carbon of the CO_2 molecule and the carbons of PFH (left), and the carbons of Hexane (right) at 298.15K.

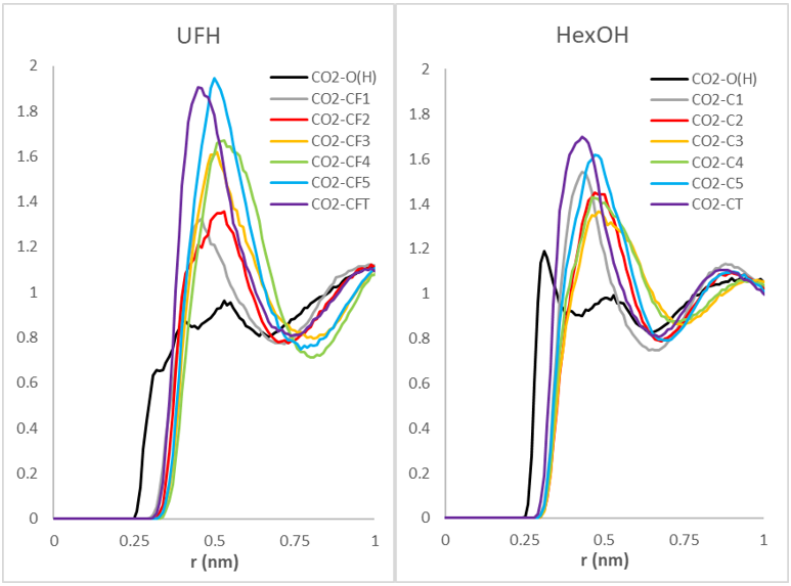

Figure 3.15: RDFs between the carbon of the CO_2 molecule and the carbons and oxygen of UFH (left), and the carbons and oxygen of hexanol (right) at 298.15K.

As can be seen, for the perfluorohexane solution the most intense peak is the CO_2-CF2 interaction, then the terminal carbons and the lowest peak is the CO_2-CF3. For the hexane the most intense peak is the CO_2-CT with the peaks decreasing along the chain. This seems to demonstrate a preference of the CO_2 molecule to being closer to the methyl group in the hydrogenated chain, this effect seems to be more preponderant in hexane than in PFH. In UFH the CO_2 molecule shows a clear preference for the end of the fluorinated chain. The most intense peaks are the CO_2-CFT and the CO_2-CF5. The intensity of the peaks decreases with the proximity to the OH group. The behaviour of the CO_2 molecule in hexanol is different as the highest peak is CO_2-CT (terminal carbon) followed by CO_2-C5, however the peaks don't decrease along the chain as it happened for the hexane. It's possible to observe that the third highest peak is the CO_2-C1, showing that CO_2 has a preference to be located at the end of the chain, tendentially near the terminal group or near the carbon bonded with the oxygen. The CO_2 atom is partially charged so it's possible that its interaction is relatively strong with the polar part of the hexanol molecule, the hydroxyl group, as can be seen by the peak demonstrated by the RDF CO_2-O(H). This way an inversion of the preferred carbons of the CO_2 molecule could occur, justifying the symmetric behaviour demonstrated.

The same procedure was done for O_2 in PFH-Hex and UFH-HexOH, containing one oxygen molecule, infinite dilution situation, at 298.15K. The RDFs obtained for the pure compounds, alkanes and alcohols, are presented in figures 3.16 and 3.17, respectively.

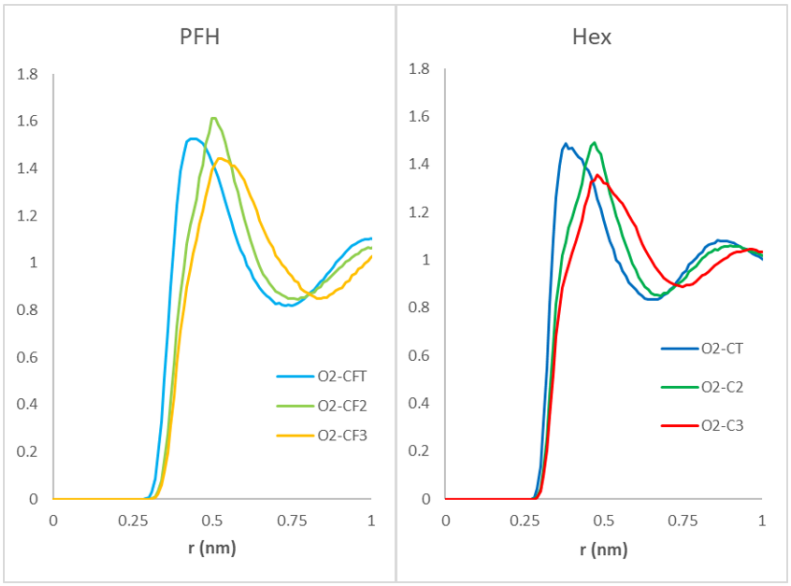

Figure 3.16: RDFs between O_2 and the carbons of PFH (left), and the carbons of hexane (right) at 298.15K.

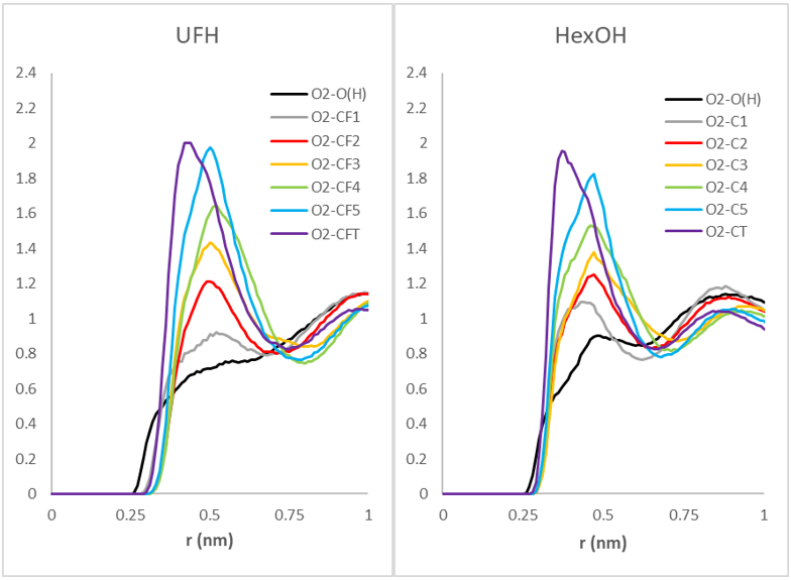

Figure 3.17: RDFs between O_2 and the carbons and oxygen of UFH (left), and the carbons and oxygen of hexanol (right) at 298.15K.

Analysing the RDFs in figure 3.16, it's noticeable that in PFH the most intense peak corresponds to the O_2-CF2 interaction and the lowest peak is the O_2-CF3. For the Hex the most intense peak is the O_2-CFT with the intensity decreasing along the chain. The oxygen molecule seems to show a preference to neighbouring the methyl groups of the hydrogenated chains and in the fluorinated chains it appears to shows a preference for the CF2 carbons instead of the terminal carbons. These results are very similar to the ones obtained for the CO_2 molecule, so the conclusions taken are the same.

In figure 3.17 it's possible to observe that the highest peak corresponds to that of the terminal group in both UFH and Hexanol (O_2-CFT and O_2-CT), a behaviour analogue to that of the CO_2 molecule in the same solvents. The peaks then decrease along the chain with the smallest peak being that of the hydroxyl group of the chain. It is also worth mentioning that the peak of the RDFs O_2-O(H) are both bellow one, meaning that the probability of the O_2 and the hydroxyl group being neighbours is very low in both alcohols. This is an indication that the O_2 molecule is preferentially located near the terminal group.

3.3.2 Location of CO_2 and O_2 in Mixtures of (Hydrogenated+Perfluorinated) Solvents

To analyse the behaviour of CO_2 and establish if there is a preference for one of the solvents in mixtures of alcohols and alkanes, RDFs CO_2-F and CO_2-H for mixtures with molar fractions of 0.25, 0.50 and 0.75 PFH or UFH at 298.15K were generated and are shown in figures 3.18 and 3.19.

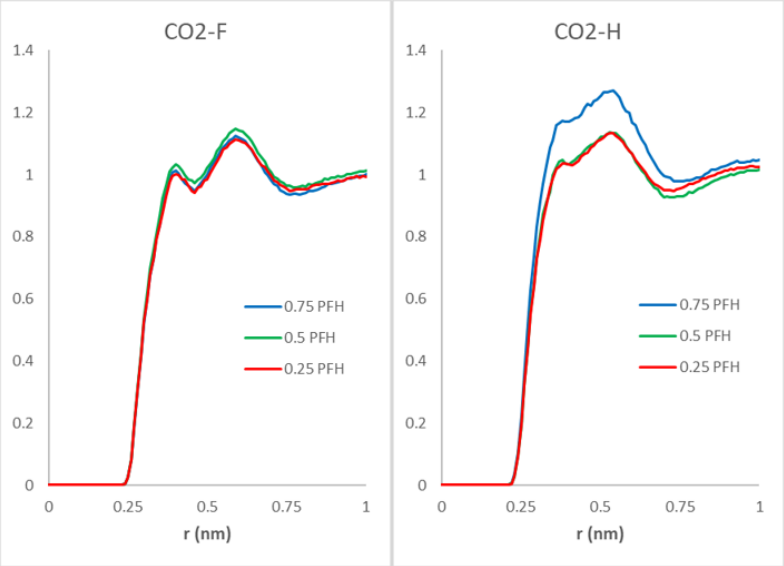

Figure 3.18: RDFs between the carbon of CO_2 and the fluorine atoms of PFH (left), and the hydrogen atoms of hexane (right) at different compositions at 298.15K.

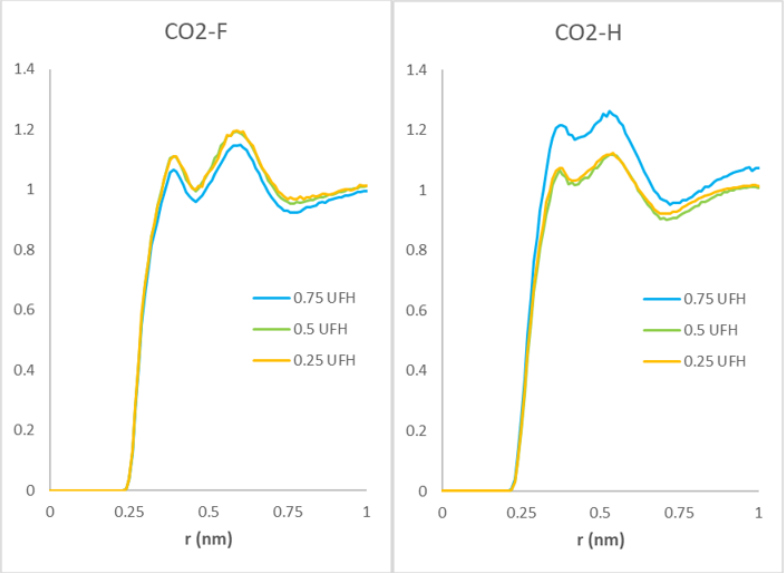

Figure 3.19: RDFs between the carbon of CO_2 and the fluorine atoms of UFH (left), and the hydrogen atoms of hexanol (right) at different compositions at 298.15K.

In figure 3.18 it's possible to see that the peaks of the RDFs CO_2-F in alkanes have very similar intensities, with the peak corresponding to the equimolar mixture being very slightly more intense. For the RDFs CO_2-H the mixture of 75% PFH has the most intense peak while for the other two compositions the RDFs are very similar. So it's evident that for the 75% PFH mixture CO_2 has a clear preference for the hydrogenated solvent. For the equimolar mixture, CO_2 seems to have a higher affinity for the fluorinated chains and for the 25% mixture no clear preference is observed. For the alcohol mixtures in figure 3.19 the same conclusion is reached for the mixture of 75% UFH, as the CO_2-H RDF peak is higher than

CO_2-F peak showing a clear preference for the hydrogenated alcohol. In the equimolar mixture, on the other hand, the CO_2 molecule seems to have a higher affinity for the fluorinated chain. The same can be conclude for the mixture of 25% UFH, even though the concentration in hydrogenated molecules is higher. It is known that fluorinated chains form more cavities than their hydrogenated counterparts [5]. This allows the allocation of the CO_2 molecules to these cavities which may help explain the apparent preference for the fluorinated chains.

The RDFs O_2-F and O_2-H were obtained for different compositions of the same mixtures, just like for the CO_2 molecule, to study the affinity of the O_2 molecule for fluorinated and hydrogenated solvents at 298.15K. The results are shown in figures 3.20 and 3.21.

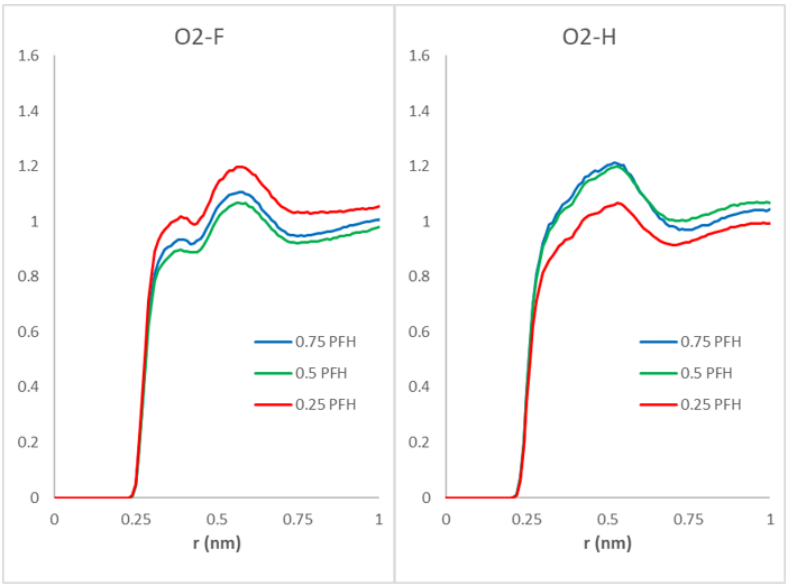

Figure 3.20: RDFs between O_2 and the fluorine atoms of PFH (left), and the hydrogen atoms of hexane (right) at different compositions at 298.15K.

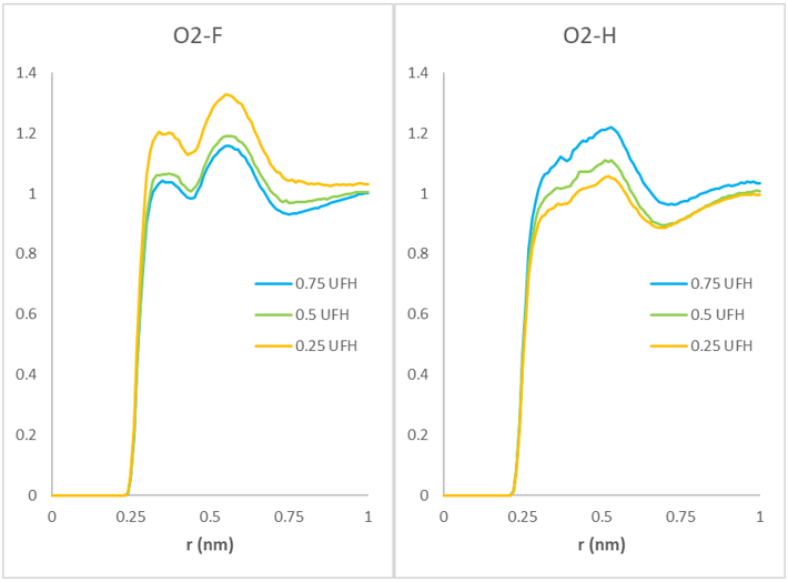

Figure 3.21: RDFs between O_2 and the fluorine atoms of UFH (left), and the hydrogen atoms of hexanol (right) at different compositions at 298.15K.

Observing figure 3.20 it's visible a higher affinity of the O_2 molecule for the hydrogenated compound in the mixture of 75% PFH. In the equimolar mixture the O_2 molecule also seems to prefer the hydrogenated chains, contrary to the behaviour of the CO_2 molecule which preferred the fluorinated

compounds. For the mixture of 25% PFH O_2 prefers the fluorinated solvent, possibly for the reason already mentioned, the formation of cavities by the fluorinated chains where the O_2 molecule can stay. For the mixture of UFH+HexOH, O_2 behaves just like in the alkane mixtures for the compositions of 25% and 75% in UFH, preferring the fluorinated and hydrogenated chains respectively. For the equimolar mixture O_2 has a higher affinity for the fluorinated compound.

3.3.3 Local Compositions

After analysing the RDFs, the local composition of the alkane and alcohol mixtures around the solute molecules was calculated. In figures 3.22 and 3.23, the difference between the bulk and the local compositions of fluorine for the alkane and alcohol mixtures are shown, respectively.

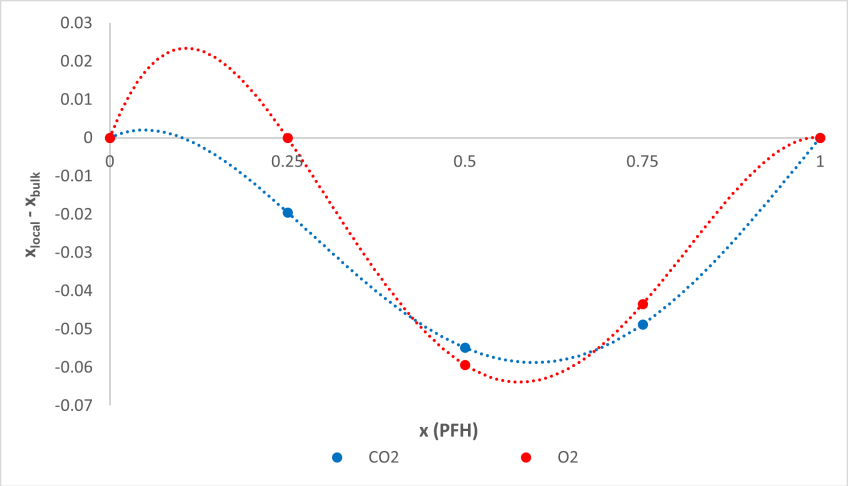

Figure 3.22: Local Enrichment of CO_2 (blue) and O_2 (red) as a function of bulk molar fraction of PFH in mixtures of PFH and Hexane at 298.15K

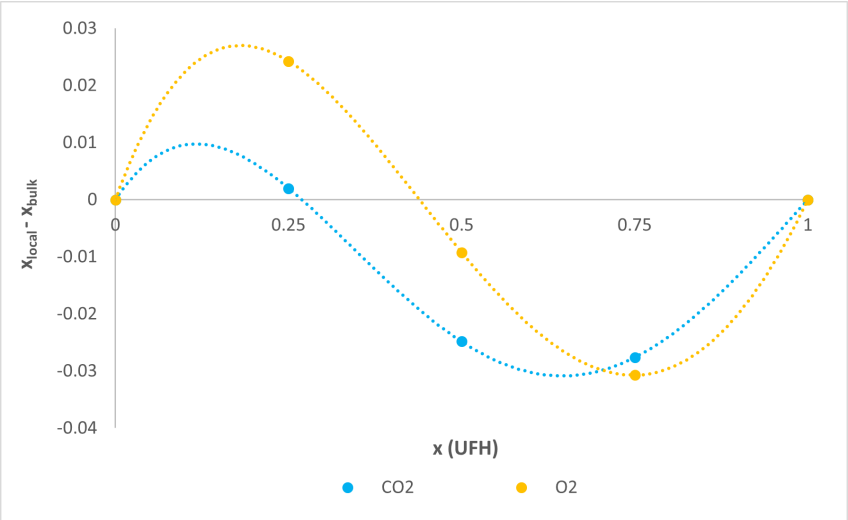

Figure 3.23: Local Enrichment of CO_2 (blue) and O_2 (yellow) as a function of bulk molar fraction of UFH in mixtures of UFH and Hexanol at 298.15K

From these figures we can see what the concentration of fluorine around CO_2 or O_2 is when compared to the bulk concentration of the mixtures. It's noticeable that the local enrichment follows a similar pattern for CO_2 and O_2. For the alkane mixtures the results show a tendency to be negative which means that the concentration in fluorine near the solute molecules is smaller than the bulk concentration

of fluorine, consequently, the hydrogen local concentration is higher than the hydrogen bulk concentration. This leads us to believe that CO_2 and O_2 appear to show a tendency to be near the hydrogenated solvent. For the alcohol mixtures we can see that these results follow a 'S' like shape being positive for the mixture with higher bulk concentration of hydrogen and negative for the other mixtures. This seems to demonstrate a preference of the solute molecules for the hydrogenated solvent in mixtures of 50% and 75% UFH and a preference for the fluorinated solvent in the mixture of 25%. When comparing both mixtures, the fluorine local enrichment in PFH+Hex is higher than in UFH+HexOH. This might result from the higher degree of nano-segregation in the alkane mixture that makes the difference in local composition more evident as the solvents are more segregated. It's important to emphasize that CO_2 and O_2 are said to be fluorophilic however from the present results that is not observed as they seem to exhibit a preference for the hydrogenated solvents.

3.4 Dynamics and Interaction Energies of Molecular Probes

The next object of this study was the movement of the particles in the mixtures previously simulated, through the analyses of diffusivity, hydrodynamic radius and interaction energies. No data was found for mixtures with the conditions of this study, so it is not possible to compare the results obtained with experimental or simulated values.

3.4.1 Solvent Dynamics

First, the diffusion coefficients of the hydrogenated and fluorinated chains in mixtures of PFH+Hex and UFH+HexOH at 298.15K were calculated, through the method explained in chapter 2.1, and they are displayed in figures 3.24 and 3.25.

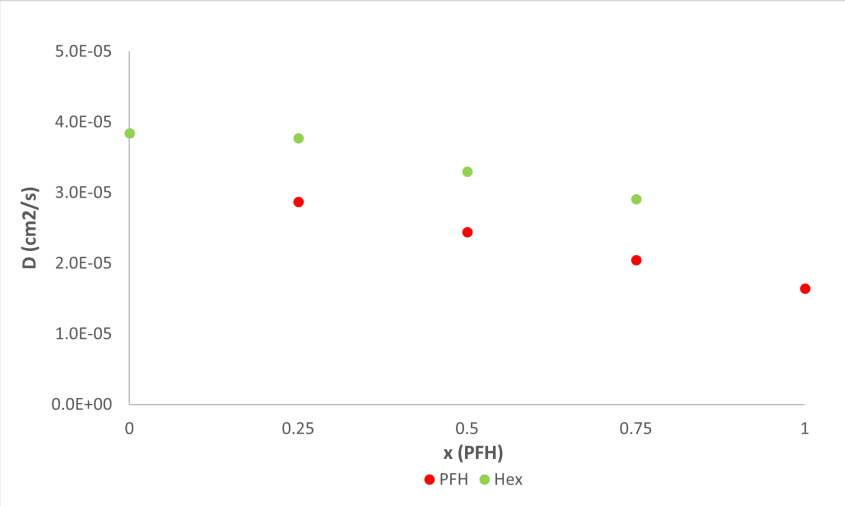

Figure 3.24: Diffusion Coefficient of PFH and Hexane in mixtures of PFH+Hex at different compositions at 298.15K

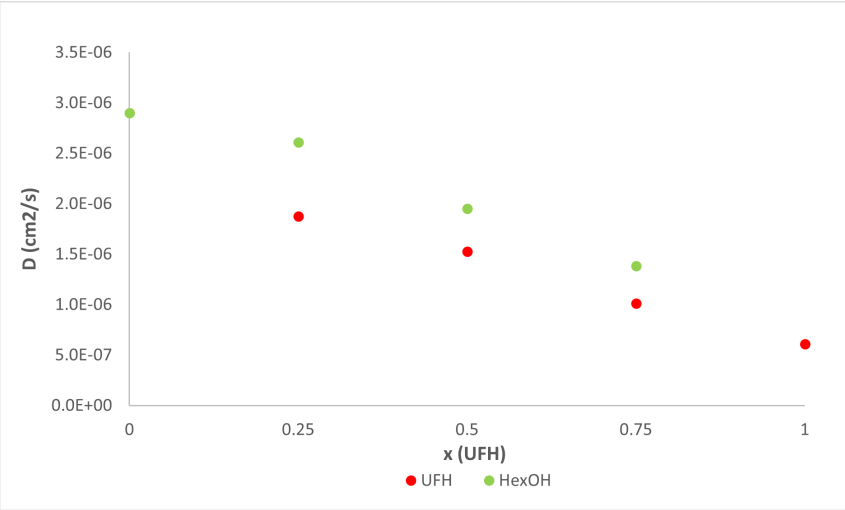

Figure 3.25: Diffusion Coefficient of UFH and Hexanol in mixtures of UFH+HexOH at different compositions at 298.15K

From the results obtained in figure 3.24 it's possible to see that the diffusivity of the hexane is higher than that of PFH, since fluorine is bigger than hydrogen it is more difficult for PFH to move through the mixture resulting in a lower diffusion coefficient. It also justifies the fact that the diffusivity of both molecules decreases with the increase of perfluorohexane in the mixtures. For the alcohol mixtures, in figure 3.25, the same conclusions are reached but it is also worth noting that these diffusion coefficients are lower than the results obtained for the alkane mixtures. A possible justification for this is the fact that the hydroxyl group in the alcohol mixtures forms hydrogen bonds, which does not happen in the alkane mixtures, constraining the movement of the molecules thus lowering their diffusivity.

To try and better understand the movement of the molecules in the mixtures studied, the hydrodynamic radius was also calculated through the Stokes-Einstein equation 2.7. This allows an analysis of the movement of the particles without the influence of the viscosity. The results obtained are shown in figures 3.26 and 3.27.

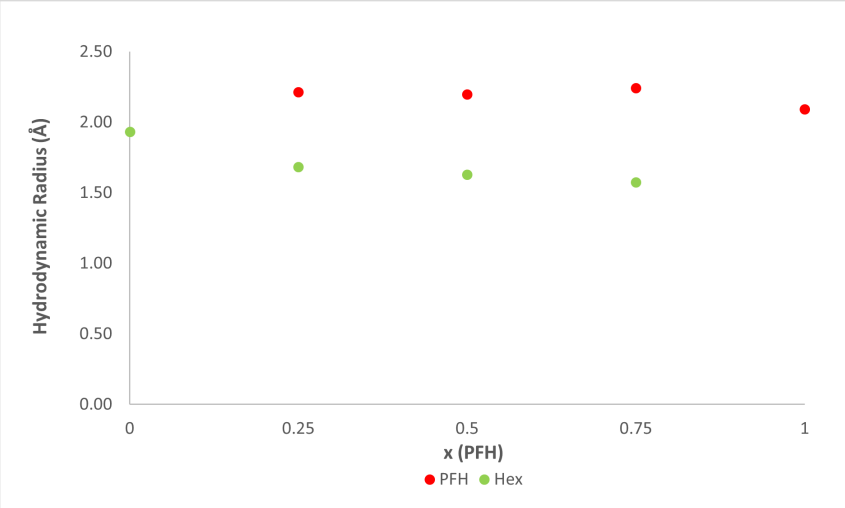

Figure 3.26: Hydrodynamic Radius of PFH and Hexane in mixtures of PFH+Hex at different compositions at 298.15K

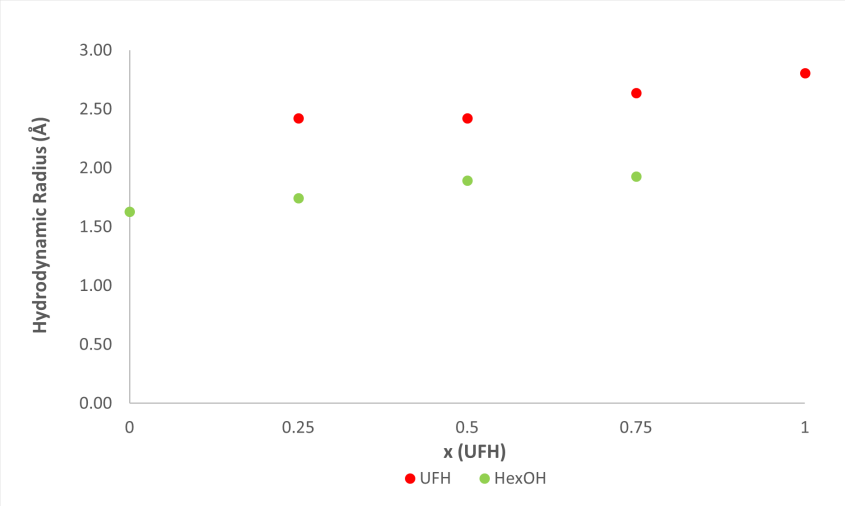

Figure 3.27: Hydrodynamic Radius of UFH and Hexanol in mixtures of UFH+HexOH at different compositions at 298.15K

Analysing the results from figure 3.26, it's possible to observe that the hydrodynamic radius of PFH is higher than that of hexane. Since a bigger hydrodynamic radius translates to a higher difficulty for the particle to move through the mixture, these results support the conclusions already reached in the analyses of the diffusivity. The PFH's hydrodynamic radius is practically constant with the increase in PFH concentration, as for hexane it slightly decreases with the increase in PFH. In the alcohol mixture, we can see that the opposite happens as the hydrodynamic radius increases with the increase in UFH concentration meaning it becomes more difficult to move through the mixture possibly due to its bigger size, as already mentioned. To the best of our knowledge there are no experimental diffusivities to compare to the results obtained. However, it is known that the experimental viscosities of these mixtures display large negative deviations, compatible with the weak interaction between hydrogenated and fluorinated chains. In light of this, the present results are not easy to understand. The results seem to indicate that in the Hex+PFH mixtures it is the hexane molecule that is responsible for the reduction in viscosity, since the hydrodynamic radius becomes smaller in the mixtures. Conversely, in the mixtures of alcohols it is the UFH molecule that moves quicker, as indicated by its hydrodynamics radii that becomes smaller.

3.4.2 Probe Dynamics and Interaction Energies in Perfluorohexane and Hexane

The same method was applied for CO_2 and O_2 to study their motion in the alkane mixtures at 298.15K. The results of their diffusion coefficients and hydrodynamic radius are respectively displayed in figures 3.28 and 3.29.

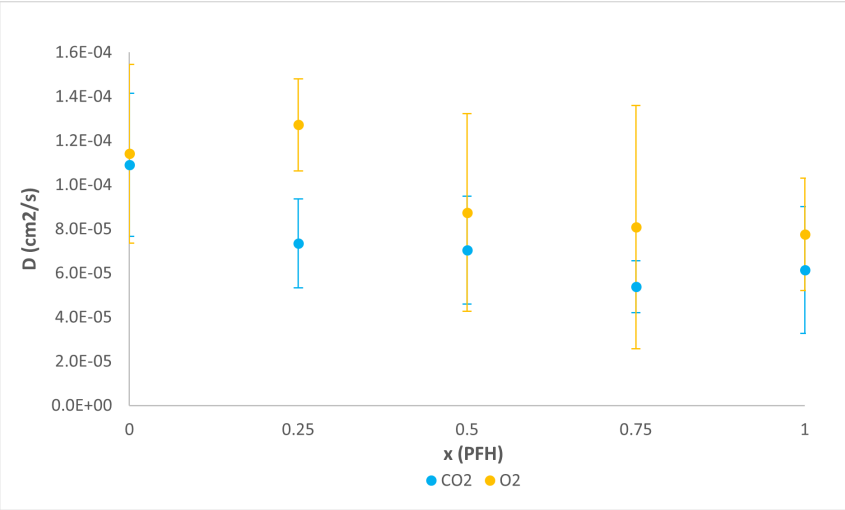

Figure 3.28: Diffusion Coefficient of CO_2 and O_2 in mixtures of PFH and Hexane at different compositions at 298.15K

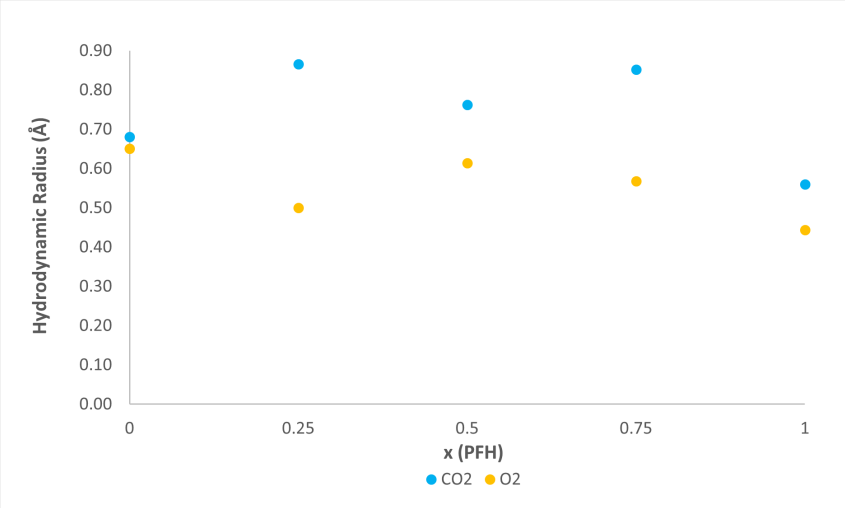

Figure 3.29: Hydrodynamic Radius of CO_2 and O_2 in mixtures of PFH and Hexane at different compositions at 298.15K

Observing the diffusion coefficients in the alkane mixtures, figure 3.28, it's noticeable that the CO_2 molecule has a lower diffusion coefficient than O_2, so it's more difficult for CO_2 to move through the mixture. Another thing that is possible to conclude is that the diffusivity overall decreases with the increase in fluorinated compound, possibly as a consequence of the increase in the viscosity of the mixture. The only exception is the diffusivity of O_2 for a composition of 25% in PFH but it fits within the standard deviation. The hydrodynamic radius of O_2 is lower than that of CO_2, agreeing with the conclusions from the analysis of the diffusion coefficients. The overall conclusion seems to be that in the mixtures the motion of CO_2 is more difficult than in the pure solvents and for O_2 its movements get easier with the increase in PFH concentration.

Since there is only one probe molecule in each system the results obtained have high statistical uncertainty associated, although the order of magnitude of the diffusion coefficients is correct. To get more exact results another method of calculation should be used or simulations of bigger systems with more solute and solvent molecules should be done to get better statistics in the MSDs, while maintaining the infinite dilution situation, resulting in a lower uncertainty associated. Once again, there are no experimental data to compare with the simulation results obtained. However, as previously mentioned, it is known that the experimental viscosities of these mixtures display large negative deviations. The

present results are thus difficult to interpret.

The interaction energies between CO_2/O_2 and the alkane solvents were determined and the results are displayed in figures 3.30 and 3.31.

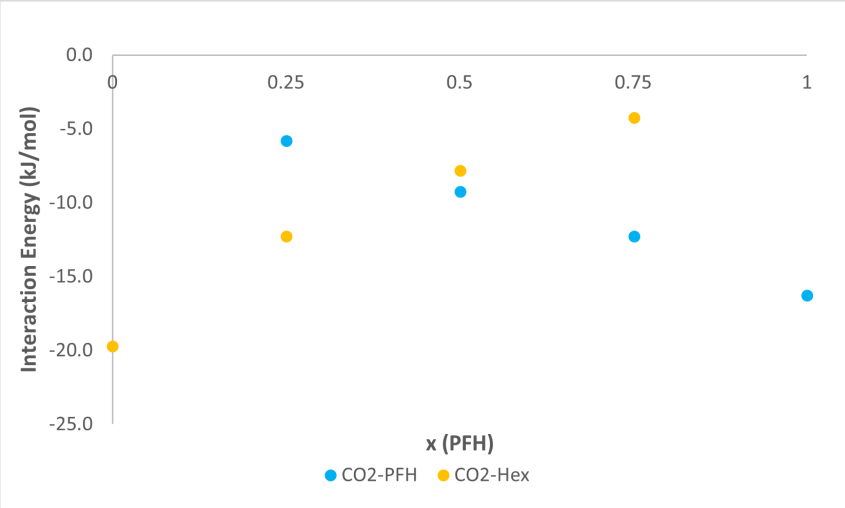

Figure 3.30: Interaction Energy of CO_2 with PFH and Hexane in Mixtures of PFH+Hex at 298.15K

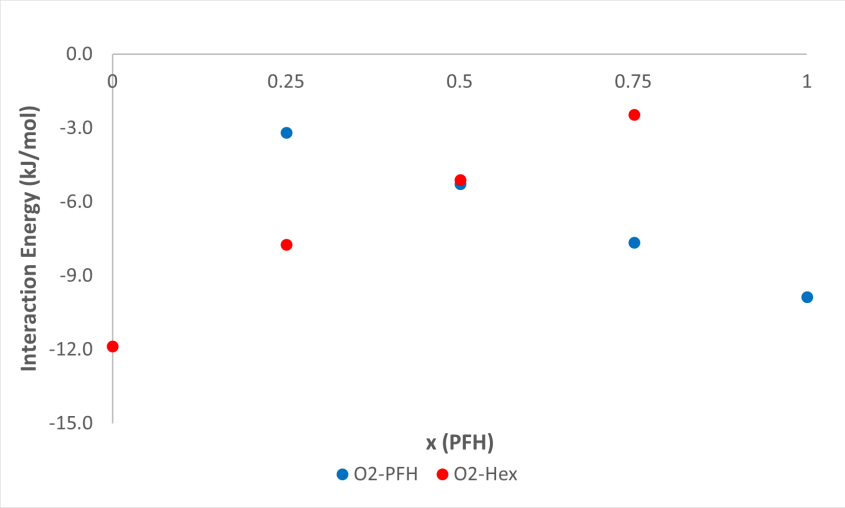

Figure 3.31: Interaction Energy of O_2 with PFH and Hexane in Mixtures of PFH+Hex at 298.15K

Examining the results obtained it's possible to note that in the pure solvents the IE is larger (more negative) between the probes and hexane, and CO_2 interacts more strongly with both solvents than O_2. This is in agreement with the results obtained for the hydrodynamic radius and diffusivities, since CO_2 interacts more strongly with the solvents it means it's more difficult for CO_2 to move through the liquid mixtures, so the diffusion coefficients are lower. Comparing the interaction energy of each probe with both pure solvents, it's possible to see that CO_2 and O_2 have a stronger interaction with Hex than with PFH, even though their diffusivity is higher in hexane. This is probably due to the contribution of viscosity in the diffusion coefficients, as the viscosity of PFH is higher than the viscosity of Hex it results in an enhanced movement of CO_2 and O_2 in hexane. As expected, the IE of both solutes vary linearly with the solvents concentration. However, a slight deviation to lower IE (less negative) can be observed for both O_2 and CO_2 with hexane, particularly at low concentration of the fluorinated component. This result is compatible with the results obtained for the local concentration of each solute.

3.4.3 Probe Dynamics and Interaction Energies in Perfluorohexanol and Hexanol

The diffusion coefficients and hydrodynamic radius of CO_2 and O_2 in the alcohol mixtures were also determined, and the results are presented in figures 3.32 and 3.33, respectively.

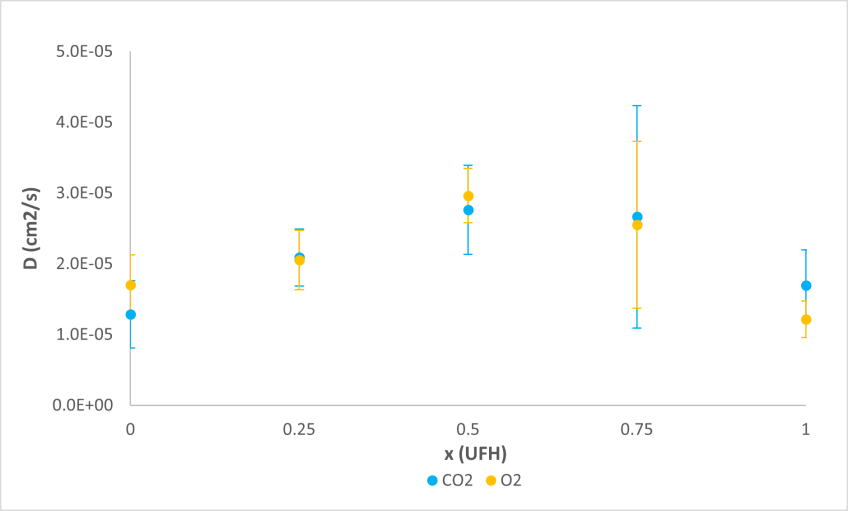

Figure 3.32: Diffusion Coefficient of CO_2 and O_2 in mixtures of UFH and Hexanol at different compositions at 298.15K

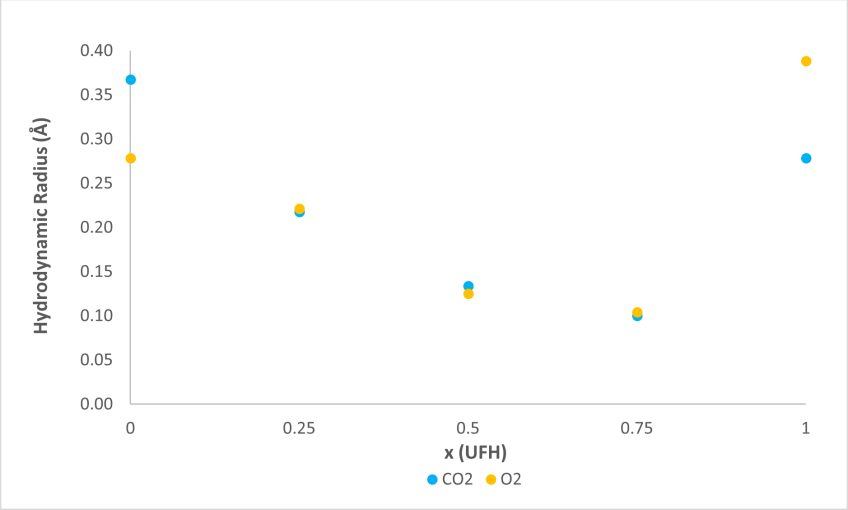

Figure 3.33: Hydrodynamic Radius of CO_2 and O_2 in mixtures of UFH and Hexanol at different compositions at 298.15K

For the UFH+HexOH mixtures it's visible that the diffusion coefficients of CO_2 and O_2 are lower than in the alkane mixtures probably due to the formation of a hydrogen bond network between the hydroxyl groups making movement more difficult for the probe molecules. Interestingly, in this case the diffusion coefficients don't decrease with the increase in UFH concentration but instead the mixtures show a positive deviation, resulting in higher diffusion coefficients than in pure solvents. In agreement, the hydrodynamic radius show a negative deviation, showing that the mobility of the probe molecules is higher in the mixtures than in pure solvents. This can be a good indication that the hydrogen bond network in the alcohol mixtures is less effective than in the pure alcohols, making the motion of the solutes easier throughout the mixtures than throughout the pure solvents.

The interaction energies between CO_2/O_2 and the alcohol solvents were also determined and the results are displayed in figures 3.34 and 3.35.

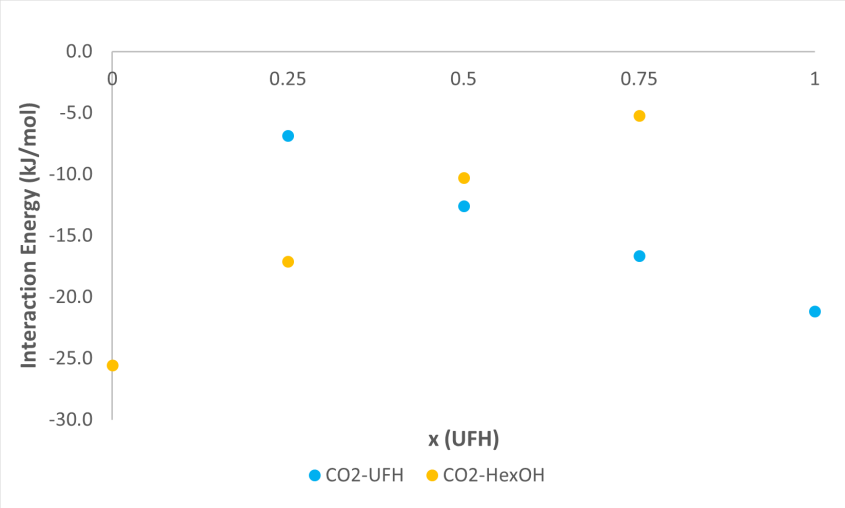

Figure 3.34: Interaction Energy of CO_2 with UFH and Hexanol in Mixtures of UFH+HexOH at 298.15K

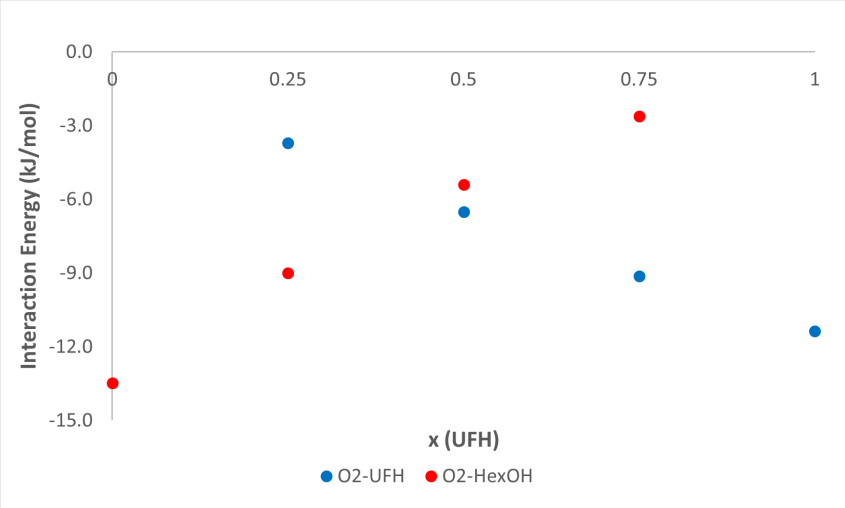

Figure 3.35: Interaction Energy of O_2 with UFH and Hexanol in Mixtures of UFH+HexOH at 298.15K

The interaction energy between CO_2 and the alcohol solvents is larger (more negative) than the IE of O_2, just like in the alkane mixtures. But the interactions with the alcohol solvents are stronger than with the alkane solvents. A possible explanation is the existence of the hydroxyl group (polar component of the solvent molecules) in the alcohols strengthening the interactions with the probe molecules. When comparing these results with the hydrodynamic radius and the diffusivity of the solute molecules, it's noticeable that CO_2 interacts more strongly with HexOH than O_2, which is reflected in the hydrodynamic radius as it is lower for O_2, meaning it moves more easily through the liquid. However, in UFH the hydrodynamic radius is higher for O_2 even though the interaction between O_2 and UFH is weaker than the interaction of CO_2 and UFH. As in the case of Hex+PFH, the IE of both solutes vary linearly with the solvents concentration. Again, a slight deviation to lower IE (less negative) can be observed for both O_2 and CO_2 with hexane, particularly at low concentration of the fluorinated component. These deviations are compatible with the results obtained for the local concentration of the solutes, although in the case of the alcohols, the differences between local concentration and nominal concentration are smaller.

Chapter 4

Conclusion and Future Work

The objectives of this work were to assess and compare the affinity of respiratory gases, in particular CO_2 and O_2, often said to be fluorophilic, towards hydrogenated and fluorinated solvents using molecular dynamics simulations as a tool. Information about the dynamics of O_2 and CO_2 solutions was also sought.

Additionally, mixtures of hydrogenated and perfluorinated fluids are known to form nano-segregated hydrogenated and perfluorinated domains, that xenon atoms are able to detect dissolving preferentially in hydrogenated environments. Following the same strategy, the ability of CO_2 and O_2 as test particles, to detect hydrogenated and perfluorinated nano-domains in mixtures of hydrogenated and fluorinated liquids, was intended, an effect that has not yet been experimentally or theoretically detected.

With these objectives in mind, a number of important conclusions could be reached.

The density and excess molar volume of the simulated mixtures of hydrogenated and perfluorinated solvents show a good agreement with experimental data. This validates the force field used to study the behavior of these mixtures. Moreover, analyses of the radial distribution functions between fluorine and hydrogen confirm the existence of nano-segregation between the hydrogenated and perfluorinated chains resulting in the formation of fluorinated and hydrogenated domains. This segregation is more evident in the mixtures of Hex+PFH, probably due to the existence of a network of H-bonds in the alcohol mixtures that decrease the effect of unfavorable dispersion forces present from the apolar part of the chains.

The Henry's constants and the solvation enthalpies of the solutes in pure hexane and PFH also reproduce well the existing experimental data, contributing to the validation of the simulations performed and more importantly validating the model used to describe the interactions between the solutes and the solvents. Moreover, the simulation results confirm that the solubility of CO_2 and O_2 in perfluorinated solvents is almost two times larger than in hydrogenated solvents.

The RDFs show that in the pure solvents, CO_2 seems to demonstrate a preference to neighbor the terminal groups of the solvents. In Hex+PFH mixtures it seems to prefer the proximity of hydrogenated groups, as CO_2 is locally enriched in hydrogen. In the UFH+HexOH mixtures, however, CO_2 seems to prefer domains enriched in hydrogenated groups for mixtures containing 50% - 75% of UFH, while for mixtures of low UFH concentration CO_2 shows a preference for fluorinated domains.

The behavior of O_2 is similar to that of CO_2 in pure solvents, exhibiting a preference for the terminal groups of the solvents. In mixtures of Hex+PFH, O_2 also seems to prefer the hydrogenated domains. For the alcohol mixtures, it also seems to prefer hydrogenated domains for compositions of 75% and 50% in UFH, and fluorinated domains for mixtures with 25% of UFH.

Thus, in general, the simulation results do not indicate any preferential location of O_2 and CO_2 towards perfluorinated solvents. On the contrary, both gases seem to dissolve preferentially within hydrogenated environments, except in a narrow range of concentration, at low fluorinated content. This result is the opposite of what could be expected since these probes are said to be fluorophilic. Xenon,

a particle that is known to be fluorophobic, is able to distinguish between hydrogenated and fluorinated domains and preferentially dissolve within the hydrogenated. Apparently, O_2 and CO_2 in spite of their enhanced solubility in fluorinated solvents, when both types of chains are present also ”prefer” hydrogenated domains. These results are in line with the interaction energies obtained in the simulations.

The enhanced solubility of the gases in the fluorinated solvents is thus probably due to the existence of cavities intrinsic to the liquid structure of the perfluorinated solvents.

Regarding the dynamics of the O_2 and CO_2 solutions, the simulated diffusion coefficients in mixtures of Hex+PFH, as could be expected, CO_2 (larger particle) has a lower diffusion coefficient than O_2, and both decrease with the increase in PFH concentration, a consequence of the increasing viscosity of the mixtures. The estimated hydrodynamic radius of the probes seems to slightly decrease with the increase in PFH concentration. The interaction energy between CO_2 and the solvents is larger (more negative) than that of O_2, and both probes interact more strongly with hexane.

As for the UFH+HexOH mixtures, the diffusion coefficients of the probe molecules display positive deviation when compared to the pure solvents. The hydrodynamic radius exhibits a negative deviation being lower in the mixtures and higher in pure solvents. This indicates that they move more quickly through the mixtures. Both probes interact more strongly with the hydrogenated compounds.

These results can be a good indication that the hydrogen bond network in the alcohol mixtures is less effective than in the pure alcohols, making the motion of the solutes easier through the mixtures than through the pure solvents.

A comment that should be made is the fact that the diffusion results have a much higher uncertainty as the statistics resulting from only one probe molecule are not very good. There is also no experimental data available to compare and assess their validity.

The validation of the simulation results was in many cases very difficult due to lack of experimental data. In other cases, the large statistical uncertainty inherent to some simulation methods also prevented reaching some of the desired conclusions. In some cases, more and longer simulation runs would be important, but were unfeasible during the available time.

The present results introduce new interesting questions that could be carried out as a follow up of this study. More in depth studies on the properties of these mixtures could be done, in particular obtaining experimental data on the diffusion coefficients. Longer simulations to obtain results with less uncertainty and at different temperatures would also be important. The experimental determination of the solubility of CO_2 in perfluorinated compounds, namely in perfluorohexane, would be very important, as there is a lack of experimental data on these solutions. Also important and interesting, would be the experimental determination of the solubility of CO_2 and O_2 in mixtures of hydrogenated and perfluorinated solvents. Equivalent studies should be carried out for different mixtures, or with other important molecules like water, xenon or nitrogen.

Bibliography

[1] D.M. Lemal. Perspective on fluorocarbon chemistry. *Journal of Organic Chemistry*, 69:1–11, 1 2004. doi:10.1021/jo0302556.

[2] P. Morgado, J. Black, J.B. Lewis, C.R. Iacovella, C. McCabe, L.F.G. Martins, and E.J.M. Filipe. Viscosity of liquid systems involving hydrogenated and fluorinated substances: Liquid mixtures of (hexane+perfluorohexane). *Fluid Phase Equilibria*, 358:161–165, 11 2013. doi:10.1016/j.fluid.2013.07.060.

[3] P. Morgado, C.M.C. Laginhas, J.B. Lewis, C. McCabe, L.F.G. Martins, and E.J.M. Filipe. Viscosity of liquid perfluoroalkanes and perfluoroalkylalkane surfactants. *Journal of Physical Chemistry B*, 115:9130–9139, July 2011. doi:10.1021/jp201364k.

[4] P. Morgado, J.B. Lewis, C.M.C. Laginhas, L.F.G. Martins, C. McCabe, F.J. Blas, and E.J.M. Filipe. Systems involving hydrogenated and fluorinated chains: Volumetric properties of perfluoroalkanes and perfluoroalkylalkane surfactants. *Journal of Physical Chemistry B*, 115:15013–15023, 12 2011. doi:10.1021/jp207567y.

[5] P. Morgado, L.F.G. Martins, and E.J.M. Filipe. From nano-emulsions to phase separation: Evidence of nano-segregation in (alkane + perfluoroalkane) mixtures using 129xe nmr spectroscopy. *Physical Chemistry Chemical Physics*, 21:3742–3751, 2019. doi:10.1039/c8cp06509h.

[6] P. Morgado, A.R. Garcia, L.M. Ilharco, J. Marcos, M. Anastaćio, L.F.G. Martins, and E.J.M. Filipe. Liquid mixtures involving hydrogenated and fluorinated alcohols: Thermodynamics, spectroscopy, and simulation. *Journal of Physical Chemistry B*, 120:10091–10105, 9 2016. doi:10.1021/acs.jpcb.6b04297.

[7] P. Duarte, M. Silva, D. Rodrigues, P. Morgado, L.F.G. Martins, and E.J.M. Filipe. Liquid mixtures involving hydrogenated and fluorinated chains: (p, , t, x) surface of (ethanol + 2,2,2-trifluoroethanol), experimental and simulation. *Journal of Physical Chemistry B*, 117:9709–9717, 8 2013. doi:10.1021/jp3105387.

[8] S. Ebnesajjad. Concise handbook of fluorocarbon gases, 2021.

[9] M.G. Freire, P.J. Carvalho, A.J. Queimada, I.M. Marrucho, and J.A.P. Coutinho. Surface tension of liquid fluorocompounds. *Journal of Chemical and Engineering Data*, 51:1820–1824, 9 2006. doi:10.1021/je060199g.

[10] Fluorocarbons. URL: https://sinlist.chemsec.org/chemical-groups/fluorinated-compounds/.

[11] G.M.C. Silva, J. Justino, P. Morgado, M. Teixeira, L.M.C. Pereira, L.F. Vega, and E.J.M. Filipe. Detailed surface characterization of highly fluorinated liquid alcohols: Experimental surface tensions, molecular simulations and soft-saft theory. *Journal of Molecular Liquids*, 300, 2 2020. doi:10.1016/j.molliq.2019.112294.

[12] Fluorocarbon applications. URL: https://www.chemeurope.com/en/encyclopedia/Fluorocarbon.html.

[13] M. Aryal, C.D. Arvanitis, P.M. Alexander, and N. McDannold. Ultrasound-mediated blood-brain barrier disruption for targeted drug delivery in the central nervous system. *Advanced Drug Delivery Reviews*, 72:94–109, 6 2014. doi:10.1016/j.addr.2014.01.008.

[14] C. Tsagogiorgas, F. Anger, G. Beck, A. Breedijk, B. Yard, and S. Hoeger. Impact of different emulsifiers on biocompatibility and inflammatory potential of perfluorohexyloctane (f6h8) emulsions for new intravenous drug delivery systems. *Drug Design, Development and Therapy*, 13:2097–2110, 2019. doi:10.2147/DDDT.S195954.

[15] J.J. Kwan, M. Kaya, M.A. Borden, and P.A. Dayton. Theranostic oxygen delivery using ultrasound and microbubbles. *Theranostics*, 2:1174–1184, 2012. doi:10.7150/thno.4410.

[16] E.P. Wesseler, R. Iltis, and L.C. Clark. The solubility of oxygen in highly fluorinated liquids 137. *Journal ofFluorine Chemistry*, 9:137–146, 1977.

[17] F.D. Evans and R. Battino. The solubility of gases in liquids 3. the solubilities of gases in hexafluorobenzene and in .benzene. *J. Chem. Thermodynamics*, 3:753–760, 1971.

[18] P. Raveendran and S.L. Wallen. Exploring co2-philicity: Effects of stepwise fluorination. *Journal of Physical Chemistry B*, 107:1473–1477, 2 2003. doi:10.1021/jp027026s.

[19] A. Cece, S.H. Jureller, J.L. Kerschner, and K.F. Moschner. Molecular modeling approach for contrasting the interaction of ethane and hexafluoroethane with carbon dioxide, 1996.

[20] A. Dardin, J.M. Desimone, and E.T. Samulski. Fluorocarbons dissolved in supercritical carbon dioxide. nmr evidence for specific solute-solvent interactions, 1997.

[21] G.G. Yee, J.L. Fulton, and R.D. Smith. Fourier transform infrared spectroscopy of molecular interactions of heptafluoro-1-butanol or 1-butanol in supercritical carbon dioxide and supercritical ethane. *The Journal of Physical Chemistry*, 96:6172–6181, 1992.

[22] C.R. Yonker. Solution dynamics of perfluorobenzene, benzene, and perdeuteriobenzene in carbon dioxide as a function of pressure and temperature. *Journal of Physical Chemistry A*, 104:685–691, 2 2000. doi:10.1021/jp992725z.

[23] M.F.C. Gomes and A.A.H. Pádua. Interactions of carbon dioxide with liquid fluorocarbons. *Journal of Physical Chemistry B*, 107:14020–14024, 12 2003. doi:10.1021/jp0356564.

[24] R.M.G. Monteiro. Nano-organization of fluorinated amphiphiles, 2020.

[25] M.P. Allen. *Computational soft matter: from synthetic polymers to proteins*. John von Neumann Institute for Computing, 2004.

[26] M.P. Allen and D.J. Tildesley. *Computer Simulation of Liquids*. Oxford University Press, 2 edition, 2017.

[27] R.H. Swendsen. *An Introduction to Statistical Mechanics and Thermodynamics*. Oxford University Press, 2012.

[28] M.A. González. Force fields and molecular dynamics simulations. *École thématique de la Société Française de la Neutronique*, 12:169–200, 2011. doi:10.1051/sfn/201112009.

[29] J.T. Chin. Molecular dynamics simulation of linear perfluorocarbon and hydrocarbon liquid-vapor interfaces, 1999.

[30] M. Abraham, B. Hess, D.V.D Spoel, and E. Lindahl. Gromacs reference manual version 2018, 2018.

[31] D.V.D. Spoel, E. Lindahl, B. Hess, G. Groenhof, A.E. Mark, and H.J.C. Berendsen. Gromacs: Fast, flexible, and free. *Journal of Computational Chemistry*, 26:1701–1718, 12 2005. doi:10.1002/jcc.20291.

[32] M. Parrinello and A. Rahman. Polymorphic transitions in single crystals: A new molecular dynamics method. *Journal of Applied Physics*, 52:7182–7190, 1981. doi:10.1063/1.328693.

[33] S. Nosé. A molecular dynamics method for simulations in the canonical ensemble. *Molecular Physics*, 52:255–268, 1984. doi:10.1080/00268978400101201.

[34] D.S. Maxwell, J. Tirado-Rives, and W.L. Jorgensen. Development and testing of the opls all-atom froce field on conformational energetics and properties of organic liquids development and testing of the opls all-atom force field on conformational energetics and properties of organic liquids. *Article in Journal of the American Chemical Society*, 4:99, 1996.

[35] E.K. Watkins and W.L. Jorgensen. Perfluoroalkanes: Conformational analysis and liquid-state properties from ab initio and monte carlo calculations. *Journal of Physical Chemistry A*, 105:4118–4125, 4 2001. doi:10.1021/jp004071w.

[36] S.W.I. Siu, K. Pluhackova, and R.A. Böckmann. Optimization of the opls-aa force field for long hydrocarbons. *Journal of Chemical Theory and Computation*, 8:1459–1470, 4 2012.

[37] K. Pluhackova, H. Morhenn, L. Lautner, W. Lohstroh, K.S. Nemkovski, T. Unruh, and R.A. Böckmann. Extension of the lopls-aa force field for alcohols, esters, and monoolein bilayers and its validation by neutron scattering experiments. *Journal of Physical Chemistry B*, 119:15287–15299, 12 2015. doi:10.1021/acs.jpcb.5b08569.

[38] R. Chitra and P.E. Smith. A comparison of the properties of 2,2,2-trifluoroethanol and 2,2,2-trifluoroethanol/water mixtures using different force fields. *Journal of Chemical Physics*, 115:5521–5530, 9 2001. doi:10.1063/1.1396676.

[39] A.A.H. Pádua. Torsion energy profiles and force fields derived from ab initio calculations for simulations of hydrocarbon-fluorocarbon diblocks and perfluoroalkylbromides. *Journal of Physical Chemistry A*, 106:10116–10123, 10 2002.

[40] J.G. Harris and K.H. Yung. Carbon dioxide's liquid-vapor coexistence curve and critical properties as predicted by a simple molecular model. *J. Phys. Chem*, 99:12021–12024, 1995.

[41] Y. Miyano. Molecular simulation with an eos algorithm for vapor-liquid equilibria of oxygen and ethane. *Fluid Phase Equilibria*, 158:1999–2028, 1999.

[42] M. Bohn, S. Lago, J. Fischer, and F. Kohler. Excess properties of liquid mixtures from perturbation theory: Results for model systems and predictions for real systems. *Fluid Phase Equilibria*, 23:137–151, 1985.

[43] W. Song, P.J. Rossky, and M. Maroncelli. Modeling alkane+perfluoroalkane interactions using all-atom potentials: Failure of the usual combining rules. *Journal of Chemical Physics*, 119:9145–9162, 11 2003. doi:10.1063/1.1610435.

[44] G.M.C. Silva, P. Morgado, P.Lourenço, M. Goldmann, and E.J.M. Filipe. Spontaneous self-assembly and structure of perfluoroalkylalkane surfactant hemimicelles by molecular dynamics simulations. *Proceedings of the National Academy of Sciences of the United States of America*, 116:14868–14873, 7 2019. doi:10.1073/pnas.1906782116.

[45] B. Hess, H. Bekker, H.J.C Berendsen, and J.G.E.M Fraaije. 3 lincs: a linear constraint solver for molecular simulations, 1997.

[46] B. Widom. Some topics in the theory of fluids. *The Journal of Chemical Physics*, 39:2808–2812, 1963. doi:10.1063/1.1734110.

[47] S.H. Jamali, A. Bardow, T.J.H. Vlugt, and O.A. Moultos. A generalized form for finite-size corrections in mutual diffusion coefficients of multicomponent mixtures obtained from equilibrium molecular dynamics simulation, 2020.

[48] Boltzmann constant. URL: https://www.nist.gov/si-redefinition/kelvin-boltzmann-constant.

[49] M.A.P.Costa. Property data and phase equilibria for the design of chemical processes involving carbon dioxide, 2017.

[50] L. Lepori, E. Matteoli, A. Spanedda, C.Duce, and M.R. Tiné. Volume changes on mixing perfluoroalkanes with alkanes or ethers at 298.15 K. *Fluid Phase Equilibria*, 201:119–134, 2002.

[51] J.O.M. Afonso. Transport properties of fluorinated surfactants: viscosity and diffusion of mixtures involving fluorinated alcohols, 2018.

[52] G.L. Pollack and J.F. Himm. Solubility of xenon in liquid n-alkanes: Temperature dependence and thermodynamic functions. *The Journal of Chemical Physics*, 77:3221–3229, 1982. doi:10.1063/1.444197.

[53] R.P. Kennan and G.L. Pollack. Solubility of xenon in perfluoroalkanes: Temperature dependence and thermodynamics. *The Journal of Chemical Physics*, 89:517–521, 1988. doi:10.1063/1.455494.

[54] R.P. Bonifácio, E.J.M. Filipe, C. McCabe, M.F.C. Gomes, and A.A.H. Pádua. Predicting the solubility of xenon in n-hexane and n-perfluorohexane: A simulation and theoretical study. *Molecular Physics*, 100:2547–2553, 8 2002. doi:10.1080/00268970210133170.

[55] A. M.A. Dias, R. P. Bonifácio, I. M. Marrucho, A. A.H. Pádua, and M. F. Costa Gomes. Solubility of oxygen in n-hexane and in n-perfluorohexane. experimental determination and prediction by molecular simulation. *Physical Chemistry Chemical Physics*, 5:543–549, 2002. doi:10.1039/b207512c.

[56] R.P.M.F. Bonifácio, L.F.G. Martins, C. McCabe, and E.J.M. Filipe. On the behavior of solutions of xenon in liquid n -alkanes: Solubility of xenon in n -pentane and n -hexane. *Journal of Physical Chemistry B*, 114:15897–15904, 12 2010. doi:10.1021/jp105713m.